Accepted Manuscript

Snow profile temperature measurements in spatiotemporal analysis of snowmelt in a subarctic forest-mire hillslope

Leo-Juhani Meriö, Hannu Marttila, Pertti Ala-aho, Pekka Hänninen, Jarkko Okkonen, Raimo Sutinen, Bjørn Kløve

PII: S0165-232X(17)30263-X
DOI: doi:10.1016/j.coldregions.2018.03.013
Reference: COLTEC 2553

To appear in: *Cold Regions Science and Technology*

Received date: 2 June 2017
Revised date: 17 January 2018
Accepted date: 12 March 2018

Please cite this article as: Leo-Juhani Meriö, Hannu Marttila, Pertti Ala-aho, Pekka Hänninen, Jarkko Okkonen, Raimo Sutinen, Bjørn Kløve , Snow profile temperature measurements in spatiotemporal analysis of snowmelt in a subarctic forest-mire hillslope. The address for the corresponding author was captured as affiliation for all authors. Please check if appropriate. Coltec(2018), doi:10.1016/j.coldregions.2018.03.013

Snow profile temperature measurements in spatiotemporal analysis of snowmelt in a subarctic forest-mire hillslope

Leo-Juhani Meriö[a*], Hannu Marttila[a], Pertti Ala-aho[a,b], Pekka Hänninen[c], Jarkko Okkonen[c], Raimo Sutinen[d], Bjørn Kløve[a]

[a]Water Resources and Environmental Engineering, PO Box 4300, 90014 University of Oulu, Finland (e-mail: leo-juhani.merio@oulu.fi, hannu.marttila@oulu.fi, bjorn.klove@oulu.fi)

[b]Northern Rivers Institute, School of Geosciences, University of Aberdeen, Elphinstone Road, Aberdeen, AB24 3UF (email: pertti.ala-aho@abdn.ac.uk)

[c]Geological Survey of Finland, PO Box 96, 02151 Espoo, Finland (e-mail: pekka.hanninen@gtk.fi, jarkko.okkonen@gtk.fi)

[d]Geological Survey of Finland, PO Box 77, 96101 Rovaniemi, Finland (e-mail: raimo.sutinen@gtk.fi)

[*]Corresponding author

Leo-Juhani Meriö, E-mail: leo-juhani.merio@oulu.fi, Phone: +358407080536

Abstract

Continuous data on spatial and temporal patterns of snowmelt rates are essential for hydrological studies, but are commonly not available, especially in the subarctic, mainly due to high monitoring costs. In this study, temperature loggers were used to measure local and microscale variations in snowpack temperature, in order to understand snowmelt processes and rates in subarctic northern Finland. The loggers were deployed on six test plots along a hillslope with varying topography (elevation and aspect) and vegetation (forest, transitional zone and mires, i.e. treeless peatlands) during two consecutive winters

(2014 and 2015). At each test plot, the sensors were installed in five locations, at two heights in a snow profile. Algorithms were developed to analyse the snowmelt rates from high-resolution snowpack temperature data. The validity of the results was evaluated using snow depth and soil moisture data from adjacent reference sensors and the results were tested using an empirical degree-day snow model calibrated for each test plot. Snowmelt rates were relatively similar in mires (median 2.3 mm d^{-1} $°C^{-1}$) and forests (median 2.6 mm d^{-1} $°C^{-1}$) with apparent inter-annual variation. The observed melt rates were highest in the highest elevation plots, in transition zone in 2014 (median 4.6 mm d^{-1} $°C^{-1}$) and southwest-facing forest line in 2015 (median 3.2 mm d^{-1} $°C^{-1}$). The timing of the modelled meltwater outflow and snowpack ablation showed good agreement with the snowpack temperature-derived estimates and the soil moisture and snow depth measurements. The simple approach used represents a novel and cost-effective method to improve the spatial accuracy of *in situ* snow cover ablation measurements and melt rates and the precision of snowmelt models in the subarctic. An open-access R-based model is provided with this paper for analysis of high-frequency snow temperature data.

Keywords: Snow temperature measurements, snowmelt variability, high resolution, low-cost, subarctic, degree-day factor.

1. Introduction

Seasonal snowmelt plays a key role in hydrological processes in high latitude catchments. It affects spring floods, low flows in early summer, groundwater recharge and soil moisture conditions (Kinar and Pomeroy, 2015; Okkonen and Kløve, 2011). Recent climate projections (IPCC, 2014) and studies (Irannezhad et al., 2016; Räisänen and Eklund, 2012; Sturm et al., 2009) indicate drastic future changes in snow cover properties and the timing of snowmelt in boreal and arctic regions. Precipitation in circumpolar areas is projected to increase (IPCC, 2014), but snowfall is indicated to decrease (Irannezhad

et al., 2016; Räisänen and Eklund, 2012). Increasing trends in air temperature and changes in the proportion of precipitation falling as snow will lead to marked alteration of hydrological conditions, with potentially severe consequences (Barnett et al., 2005).

The spatiotemporal distribution of snow and its inter-annual variability are considerable (Liston and Sturm, 1998; Rasmus, 2005), mainly depending on climate conditions, topography and vegetation (Liston, 2004; Vajda et al., 2006; Winstral and Marks, 2014). Canopy cover affects snow accumulation (Pomeroy et al., 2002) and melt rates (Talbot et al., 2006), as it can intercept snow and influences e.g. the radiation balance (Luce et al., 1999) and sensible and latent heat transfer between snowpack and atmosphere (Link and Marks, 1999). In areas with subtle topography, the vegetation cover can be the primary control of snow variability (Link and Marks, 1999) and melt rates (Gelfan et al., 2004). The high small-scale variability of snow cover makes it difficult to determine the amount of snow and melt rate with reasonable measurement efforts. Furthermore, snowmelt rate should be measured in multiple locations for different topography and vegetation, even in small catchments (Kumar et al., 2016).

Kinar and Pomeroy (2015) and Lundberg et al. (2010) present an extensive review of current techniques and devices for near-surface snowpack measurements. In the past, snow depth and snow water equivalent (SWE) during snow accumulation and melt have been measured with snow stakes and lines (Kinar and Pomeroy, 2015; Kuusisto, 1984). These techniques provide essential *in situ* information on local snow depths and SWE, but are labour-demanding and unable to provide representative data for surrounding physiographical conditions (Rice and Bales, 2010). Ground penetrating radar can be used to achieve improved spatial coverage, but this method is also labour-demanding and less precise than other *in situ* techniques (Sutinen et al., 2012; Vajda et al., 2006). Automatic pressure sensors, such as snow pillows, lysimeters and acoustic sensors, have improved the temporal resolution of data, but are too costly to

provide full spatial coverage. The recent development of remote sensing techniques, such as airborne laser scanning and ranging, photogrammetry and satellite sensors, has opened up new possibilities for obtaining spatially representative data on snow cover (Bair et al., 2016; Bokhorst et al., 2016; Bühler et al., 2015; Cohen et al., 2015; De Michele et al., 2016; Leinss et al., 2015; Nolin, 2010; Sturm, 2015), but the data always require *in situ* validation (Kinar and Pomeroy, 2015). There is thus a need for a new, simple and robust measurement methods, especially to produce point and spatially comprehensive snow melt rate estimates.

Small temperature loggers placed in the snowpack or buried under the soil surface have been used to establish point measurements with large spatial coverage for snow depth and cold content (Fujihara et al., 2017; Reusser and Zehe, 2011), areal snow cover (Cunningham et al., 2006; Gottfried et al., 2002; Lundquist and Lott, 2008; Raleigh et al., 2013), snow temperature gradients (Molotch et al., 2016) and snow cover distribution (Fujihara et al., 2017; Lundquist and Lott, 2008). However, to our knowledge, temperature sensors placed in the snowpack have not been used previously to study micro- and local-scale variations in snow melt rates.

In this paper, we studied local and microscale variations in snow ablation timing and snowmelt rates in the subarctic boreal zone using snowpack temperatures measured with temperature loggers. We developed improved algorithms to analyse high-resolution temperature data from snowpack to estimate snow melt rates and ablation day in various boreal landscapes. Our main research questions were: i) Can the snowpack temperature data from low-cost temperature loggers be used to determine snow melt rates and their variability? ii) Can the drivers affecting local-scale spatiotemporal variations in ablation in a forest-mire hillslope be identified? and iii) How well do the estimated snow melt rates perform with a simple degree-day snow model?

2. Materials and methods

2.1 Study area

The experiment was conducted in a subarctic area in Pallas-Ylläs National Park in northern Finland, near the Sammaltunturi and Mustavaara mountains (Fig. 1), during two consecutive winters (2013/2014 and 2014/2015). The Köppen-Geiger climate classification system places the area in class Dfc (cold climate without dry season and cold summers; Peel et al., 2007). Vegetation in the area is mainly coniferous forest, consisting of Norway spruce (*Picea abies* (L.) *H. Karst*) and occasional Scots pine (*Pinus sylvestris* L.), downy birch (*Betula pubescens* Ehrh.) and mountain birch (*Betula pubescens* ssp. *czerepanovii*), whereas the upper slopes of the fells are treeless, containing only ground vegetation (Sutinen et al., 2012). Mean annual temperature during the period 1981-2010 ranged between -2 °C and -1 °C and mean annual precipitation between 500 mm and 550 mm, based on meteorological dataset interpolated for the whole of Finland (1 km^2 grid). (Pirinen et al., 2012). Average areal snow depth on 31 March in the period 1981-2010 was 60-80 cm and the average number of days with snow cover was 205-225 (FMI, 2015). Mean annual temperature at the Kenttärova weather station (Fig. 1), which is operated by the Finnish Meteorological Institute (FMI), was 0.6 °C in 2014 and 1.0 °C in 2015 and mean annual precipitation was 601 mm and 672 mm, respectively. Mean annual temperature and precipitation in the study area were thus markedly higher during the study years than in the period 1981-2010. Average areal snow depth on 15 March in 2014 and 2015 was between 75 and 100 cm (FMI, 2016). Number of snow days at Kenttärova station was 219 in winter 2013/2014 and 213 in 2014/2015. Areal snow depth was at the higher end or exceeded the 1981-2010 range, whereas the number of snow days was within the same range. Global shortwave radiation and cloudiness measurement data used in inter-annual analysis of the melt rates were acquired from FMI's Sammaltunturi and Kenttärova weather stations, respectively. We used climate data mainly from Kenttärova station because the sensors were located

above spruce forest at 347 m above sea level (a.s.l.), thus representing conditions better in our study area than the Sammaltunturi station, located on the top of the bare fell at 565 m a.s.l.

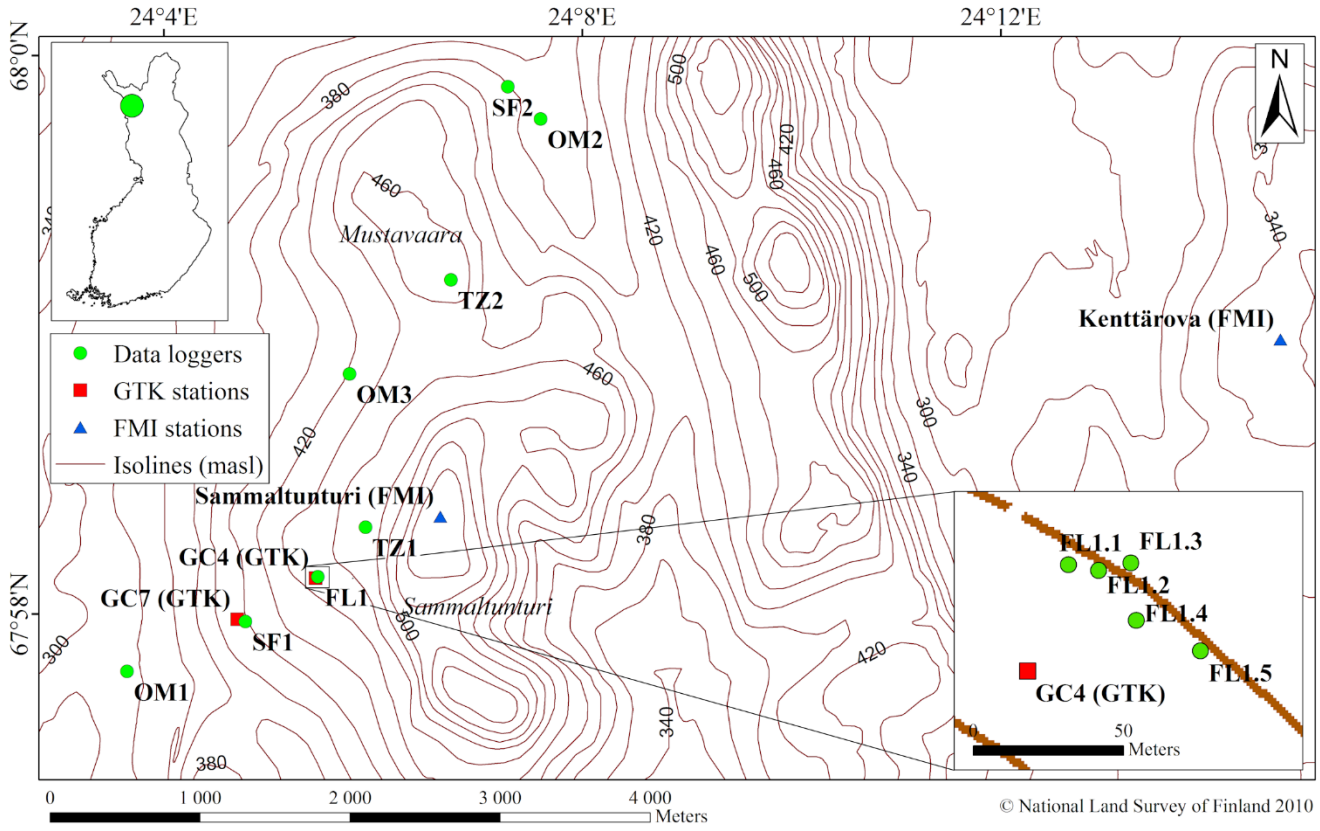

Figure 1. Study area and location of experiment plots, Geological Survey of Finland (GTK) acoustic snow reference measurements and Finnish Meteorological Institute (FMI) weather stations. The area of the forest line (FL1) test plot is expanded in the lower right corner.

2.2 Experiment locations and setup

Eight different experiment plots (Fig. 1, Fig. 2) with varying topography and vegetation were established (Table 1). Four of the plots were used in both winters and four plots in one winter. The elevation of the test plots varied from 320 m a.s.l. to 480 m a.s.l. and they were located in open mires (OM1-OM3), spruce forest (SF1, SF2), forest line (FL1), transition zone on the slope (TZ1) and next to bare fell (TZ2),

with different topographical aspects and inclinations (Table 1, Fig. 1). Canopy coverage (Table 1) was estimated using digital camera pictures taken skyward from the ground (Korhonen and Heikkinen, 2009).

Table 1. Topographical and vegetation details for measurement and reference sites. Vegetation: open mire (orange), forest/forest line (green), transitional zone (yellow). Aspect factor was calculated from slope aspect in degrees. Topography data were extracted from a 10-m digital elevation model (DEM) taken from the topographical database of the National Land Survey of Finland (2013)

Site	Vegetation	Elevation (m a.s.l.)	Inclination (degrees)	Aspect (degrees)	Aspect factor[1]	Canopy Coverage (%)
OM1	Open mire (flat fen)	320	1	270	4	0
OM2	Open mire (flat fen)	375	1	70	5	0
OM3	Open mire (sloping fen)	420	5	290	4	0
SF1 / GC7	Spruce forest	400	5	240	2	17.1
SF2	Spruce forest	380	6	45	7	21.6
FL1 / GC4	Forest line	450	5	220	2	6.2
TZ1	Open slope (transitional woodland/ shrub)	475	4	270	4	0
TZ2	Tree line (next to bare fell)	480	5	170	1	5.1

[1]1 = south, 2 = southwest, 3 = southeast, 4 = west, 5 = east, 6 = northwest, 7 = northeast, 8 = north

At each of the test plots, the temperature sensors were placed at five points and two heights in the snow column (on the ground and at a fixed height of 30 cm above the ground). The height of the upper sensor was marked with a wooden stick. The distance between the test points within plots was approximately

10-50 m (Fig. 1), which can be defined as microscale, whereas the distance between the test plots was approximately 500-4000 m, which is considered local (meso) scale (Gray, 1978; Kuusisto, 1984; Rasmus, 2005). The loggers were installed in the snowpack on 16-17 April 2014 and 24-25 February 2015 in winter 2013/2014 and 2014/2015, respectively. To minimise disturbance of the snowpack, the snow pit was kept as small as possible and the loggers were placed in a small cavity on the wall of the pit. Additional loggers were installed to record air temperature. These sensors were attached to a tree at approximately 2 m above ground level and protected from solar (shortwave) radiation with white plastic lids. In test plots SF1 and FL1, the air temperature was measured in adjacent measurement stations GC7 and GC4 (Fig. 1) operated by the Geological Survey of Finland (GTK). Snow water equivalent was determined at each test point during installation by measuring snow depth and density through taking snow cores (Table 2). The SWE values measured in spring 2014 were close to the maximum value, whereas the values measured in 2015 were taken at a time when the snow was still accumulating. The sensors were collected in summer 2014 and 2015, after all the snow had melted.

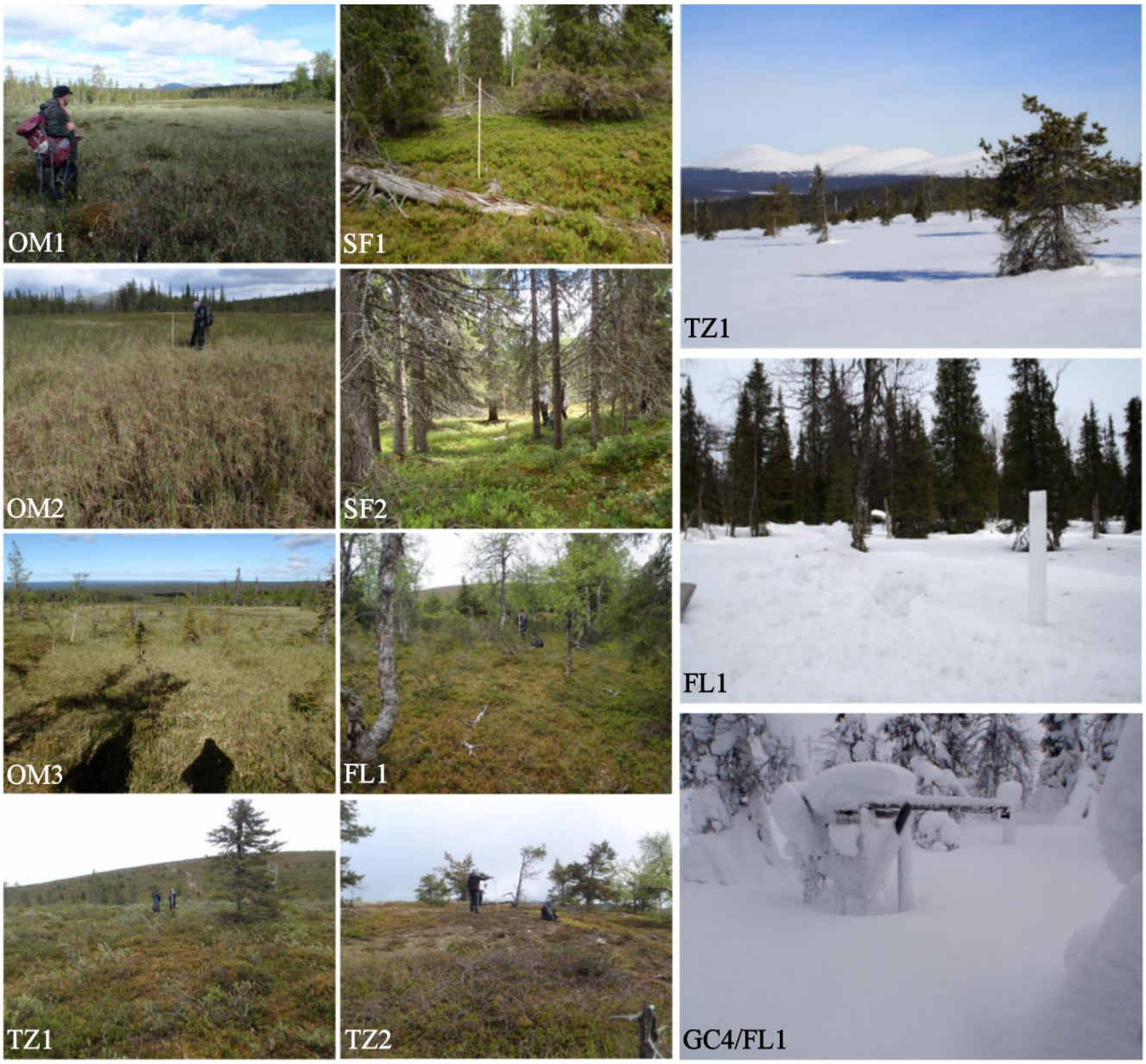

Figure 2. Test plots at Sammaltunturi and Mustavaara at the time of logger collection in summer: Open mires (OM1-OM3), spruce forest (SF1, SF2), forest line (FL1), transition zone on the slope (TZ1) and next to bare fell (TZ2). Winter pictures from TZ1 and FL1 in winter 2013/2014 and GC4/FL1 in winter 2014/2015 taken at the time of logger installation.

Table 2. Average snow depth, snow density and snow water equivalent (SWE) for each test plot, measured on 16-17 April 2014 (close to maximum value) and 24-25 February 2015 (during accumulation period). CV (coefficient of variation) = standard deviation of the sample divided by its mean.

Site	Environment type	Snow depth[1] (m)	CV[1]	Snow density[1] (kg m^{-3})	CV[1]	SWE[1] (mm)	CV[1]
OM1	Open mire (flat fen)	NA/0.65	NA/0.09	NA/234	NA/0.07	N/152	NA/0.13
OM2	Open mire (flat fen)	0.81/0.70	0.09/0.13	280/247	0.18/0.10	229/173	0.26/0.21
OM3	Open mire (sloping fen)	NA/0.60	NA/0.14	NA/239	NA/0.11	NA/143	NA/0.15
SF1	Spruce forest	0.79/0.81	0.10/0.01	287/229	0.02/0.08	227/186	0.10/0.09
SF2	Spruce forest	0.89/0.82	0.06/0.06	271/243	0.15/0.06	241/200	0.15/0.10
FL1	Forest line	0.91/0.94	0.08/0.06	290/233	0.07/0.08	265/220	0.14/0.13
TZ1	Open slope (transitional woodland/ shrub)	0.83/NA	0.21/NA	306/NA	0.10/NA	256/NA	0.30/NA
TZ2	Tree line (next to bare fell)	0.89/NA	0.17/NA	322/NA	0.08/NA	289/NA	0.21/NA
ALL[2]		0.85/0.75	0.13/0.18	293/238	0.12/0.08	251/179	0.21/0.20

[1]First value is from spring 2014 and second from winter 2015.
[2]Corresponds to the average of the test plots for each year.

2.3 Temperature measurements and data

Waterproof Onset Hobo Pedant model UA-001-08 (Onset, 2015) temperature data loggers were used to record the snow temperature profiles. The accuracy of the sensor is ±0.53 °C from 0 °C to 50 °C but decreases to ±0.8 °C at -20 °C, which is the lower end of the measurement range (Onset, 2015). A rubber cover was used to protect the logger circuit board from moisture and UV radiation. The temperature

loggers were set to record the temperature at 15-min intervals from 19 April to 16 June 2014. During the following winter, the loggers were set to record at 30-min intervals from 28 February to 27 June 2015, with the longer interval due to the longer measurement period. Sharp temperature peaks exceeding air temperature were observed during daytime in spring and were assumed to be caused by solar radiation. To minimize the error between logger and its ambient temperature, these peaks were filtered so that at air temperatures greater than 0.2 °C AND logger temperature higher than air temperature, the logger temperature was taken to be the air temperature.

2.4 Reference measurements

The measurements were compared against daily data from SR50A acoustic snow depth sensors (Campell Scientific, 2016) at measurement stations GC7 and GC4 (Fig. 1, Fig.2 GC4/FL1), adjacent to the SF1 and FL1 test plots. The measurement range of these sensors is 0.5-10 m, accuracy is 0.4% of the distance to target and resolution is 0.25 mm. Reference data were not available after 25 May in spring 2015. Water content of the soil was measured at the reference stations using CS615 TDR (time domain reflectometer) probes installed at 20 cm below ground (Sutinen et al., 2009, 2008). Daily soil moisture data were used to validate the snowmelt simulations with an empirical snow model (see Appendix A).

2.5 Detection of the time when the logger is free of snow

Changes in diurnal temperature fluctuations of the measurements can be used as the primary criterion to determine when the sensor is free of snow (Fujihara et al., 2017; Reusser and Zehe, 2011). This method is based on the high insulation properties of snow, which dampen the temperature variations in snowpack. The accuracy of the temperature sensor, the insulating properties of the snowpack and the magnitude of fluctuation of air temperature influence the accuracy of detection of the date when the logger is snow-free. In this study, 2.0 °C was used as the threshold for the standard deviation of the diurnal sensor

temperature and values between 1.5 and 2.3 °C were found to be usable in the sensitivity analysis. In a study in Japan, Fujihara et al. (2017) used 0.3 °C, which can lead to high error because the temperature of the sensor starts to fluctuate beyond this threshold before it is uncovered from the snowpack. The logger was also assumed to be free of snow in situations when the *minimum* daily temperature of the sensor was above 0.6 °C (approximately the accuracy of the sensor) even if the diurnal temperature fluctuation was below the threshold. Conversely, when the air temperature was low but the diurnal fluctuation was high, the logger was assumed to be free of snow only in situations when the *maximum* daily temperature of the sensor was above 0.6 °C simultaneously with the temperature fluctuation. Otherwise, fluctuations around sub-zero temperatures inside the snowpack could impair the detection when a cold spell is followed by a melt period that decreases the thickness of the insulating layer of snow on top of the logger.

2.6 Melt rate estimation

Degree-day factor (ddf) is a commonly used empirical factor that relates the amount of snow/ice melt, measured in SWE [mm], to mean air temperature in a specified period. It is easy to apply to a snow model, requiring only air temperature and precipitation as input data. Degree-day factor has a solid physical basis, as approximately three-quarters of the energy sources for snow/ice melt are usually related to air temperature (Hock, 2003; Ohmura, 2001). The degree-day factors were calculated for each test point using eq. (1):

$$ddf_{calc} = \frac{(h_{300} - h_0) \times \frac{\rho_s}{\rho_w}}{t_{melt} \times (T_{a\_mean} - T_m)} \quad (1)$$

where h_{300} = 300 mm is the snowpack thickness when the upper logger was revealed and h_0 = 0 mm when the lower logger was revealed, T_{a_mean} is the mean air temperature for the period (t_{melt}) when snow had melted from h_{300} to h_0, ρ_w = 1000 kg m^{-3} is the density of water, ρ_s is the snow density

during the melt, assumed to be 329 kg m^{-3} in forested areas and 349 kg m^{-3} in open areas (Kuusisto, 1984), and T_m = 0 °C is the melting threshold temperature of snow. The measured average snow density before the onset of the snowmelt in 2014 was 292.8 kg m^{-3}, and by assuming further snow compaction as the melt progresses (Bormann et al., 2013; Kuusisto, 1984) these literature values specific for the region appear reasonable. Furthermore, the calculated ddf's are averaged for the period of final 30 cm of snowmelt assuming that density changes at this point are minimal.

2.7 Performance of melt rates

The performance of the melt rates was tested using an empirical snow model (Fig. 3; see Appendix A) (DeWalle and Rango, 2008). The algorithms for high resolution temperature data analysis and snow model were implemented in R (version 3.3.1; R Foundation for Statistical Computing, Vienna, Austria) and are provided as supplementary material (Appendix B).

The model was calibrated manually against measured SWE data (accumulation period) and the date when the snowpack was estimated to be completely melted (melt period) derived from the temperature logger data. The correction factor and critical temperature for snow precipitation (Eq. A.1) were observed to have the highest impact in calibration of the *accumulation period*. They were adjusted to minimise the error between the modelled and measured SWE, as the snow accumulation processes were highly variable and the precipitation measurement point (Kenttärova) was located approximately 6 km east of the study area (Fig. 1). A linear relationship was determined between measured SWE [mm] and correction factors for snowfall at each test point by maximising Nash-Sutcliffe model efficiency (Krause et al., 2005) and minimising the bias (Kokkonen and Jakeman, 2001) between the modelled and measured SWE as the criterion for fitting the equation. For the winters 2013/2014 and 2014/2015, the resulting equations for snow precipitation correction factors were:

$$CF_{s(13/14)} = 0.0038 \times SWE_{meas} + 0.14 \quad (2)$$

$$CF_{s(14/15)} = 0.0053 \times SWE_{meas} + 0.025 \quad (3)$$

Using this procedure, the snow precipitation correction factor integrated all the accumulation and redistribution processes in a point. For the *melt period*, a scaling coefficient for the calculated degree-day factors was introduced, because the calculated ddf value represented the melt rate at the end of the snowmelt season, and the ddf was set to increase linearly from 1 Sep to 31 May because the ddf is known to increase during the melt period. The scaling coefficient and the threshold temperature for the snowmelt (Eq. A.4 and A.4.1) were adjusted to minimise the root mean square error (RMSE) (Legates and McCabe Jr., 1999) between the modelled and measured end date of the snow as the primary criterion for the melt period. The sequential process involved iterations between the calibration of accumulation and melt period, because parameters of Eq. A.1 and Eq. A.4 were found to be interdependent. During the initial model testing, the coefficients for cold content (Eq. A.5), snow surface temperature (Eq. A.6) and liquid water-holding capacity (Eq. A.7) showed no sensitivity and were fixed. The full set of calibrated and measured parameters is presented in Appendix A.

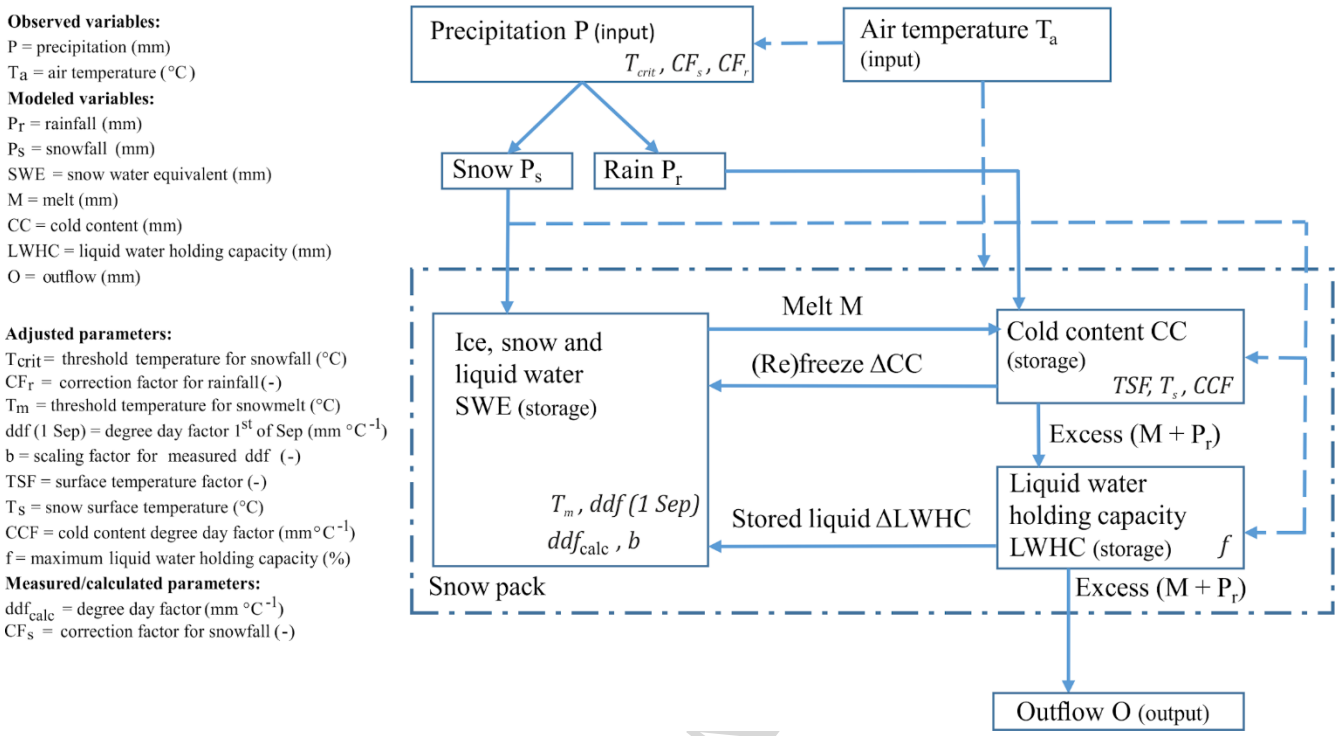

Figure 3. Flowchart of the snow model used for analysing the performance of the calculated melt rates.

3. Results and discussion

3.1 Timing and variability of snowmelt

3.1.1 Diminishing snow cover based on temperature sensor information

Timing of snowmelt among sensor locations was efficiently detected using the algorithm developed (Figs. 4a and 4b). Under the snow cover the variability in logger temperature was minor, as expected because of the high insulation properties of snow, and started to follow air temperature when exposed (e.g. Reusser and Zehe, 2011). In its current form, the method detects the first date when the criteria is fulfilled and needs further improvement to detect the correct date in case of oscillation of the snow depth above and below the logger position, which was not the case during our study period. Reasonable agreement was observed between the snow depth at the adjacent reference station and the date when the temperature variation started and when the snow cover disappeared from the respective loggers (dashed

lines in Fig. 4). The difference in snowmelt timing between SF1.1 and the reference site GC7 was most likely due to microscale variations in snow accumulation and melt speed, due to mainly small-scale variations in topography and vegetation (e.g. Jost et al., 2007). Reference measurements were assumed to be disturbed by movement of the supporting structure showing small fluctuations in the snow depth, and the underbrush, which prevented the snow depth reaching zero cm (Fig. 4).

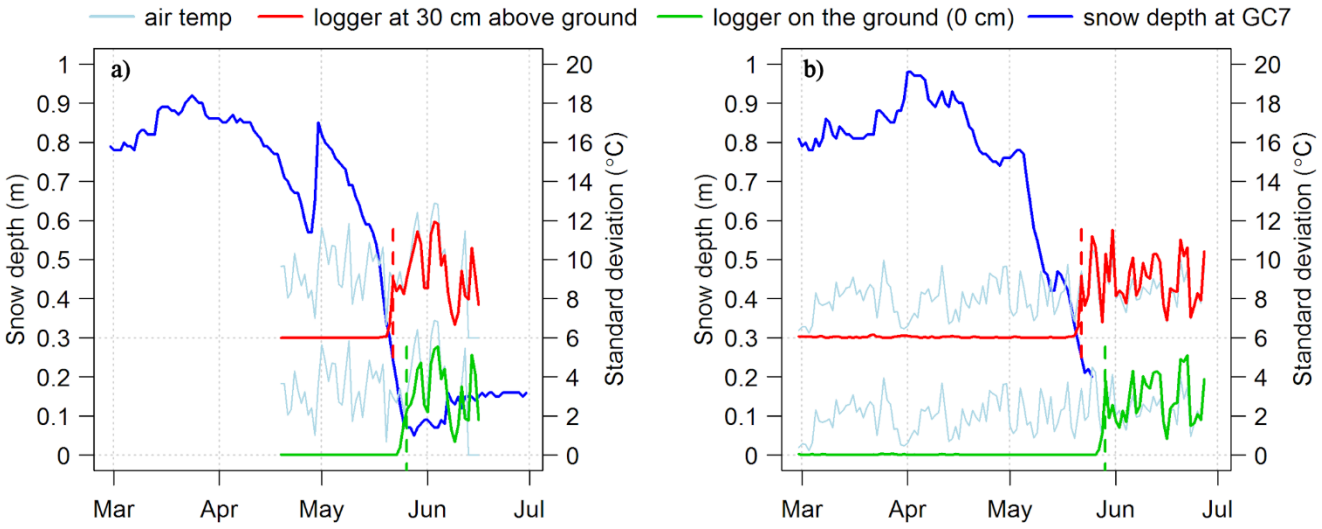

Figure 4. Diurnal standard deviation in logger temperature (red, green, light blue) at site SF1.1 and snow depth at the reference measurement station GC7 (blue) in (a) 2014 and (b) 2015. Logger temperature data at a height of 30 cm have been offset to 30 cm snow depth to visualise the logger position in the snowpack. Dashed vertical lines (red, green) mark the date when the loggers were determined to be free of snow.

3.1.2 Variability in snowmelt rates and snow ablation dates

While microscale variability and local-scale processes are often difficult to distinguish due to high small-scale variability in snow accumulation and ablation (Jost et al., 2007), our method successfully revealed the variation between and within the test plots (Fig. 5). Snow was typically observed to melt earlier in

open mires (OM1, OM2 and OM3) and areas with non-existing (TZ1) or very low canopy cover (TZ2) (Fig. 5). During both years, the snow was observed to melt last on the forested north-facing slope (SF2), which is protected from solar radiation by the topography. The early melt on open mires can be partly explained by the accumulated SWE (Liston, 1999; Lundquist and Lott, 2008), which was typically lowest for open mires, particularly in 2015 (Table 2). The reason for lower SWE on mires can be a slushing effect of snow during the start of the snow cover, as the ground stays unfrozen later than surrounding areas, because of high heat capacity of water compared to mineral soil and the groundwater supply in groundwater dominated mires (fens). Moreover, the open areas tend to accumulate less snow (e.g. Gelfan et al., 2004). This confirms previous findings for snowmelt on mires (Koskinen et al., 1997; Kuusisto, 1984).

An annual comparison was made using data from test plots SF1, SF2, FL1 and OM2, in which measurements were taken during both study winters. The average date for snow cover depletion was 27 May (range 10 days, 23 May-2 June) in 2014 and 28 May (range 8 days, 24 May-1 June) in 2015. The snow in the test area melted later than the average end date of permanent snow cover in the region in the period 1981-2010 (FMI, 2015), which was expected due to the higher elevation of the study area compared with the surrounding region. During 2014, the variation in snow cover depletion was lowest in the open mire and highest in the forested sites, while in 2015 the trends were inconsistent. In most test plots, the variation in melt time was higher at 30 cm above the ground than at ground level. The overall duration of snow depletion (Fig. 5) was higher than within a plot, which was expected as the variability of snow cover increases with scale (Shook and Gray, 1996) and between land cover types.

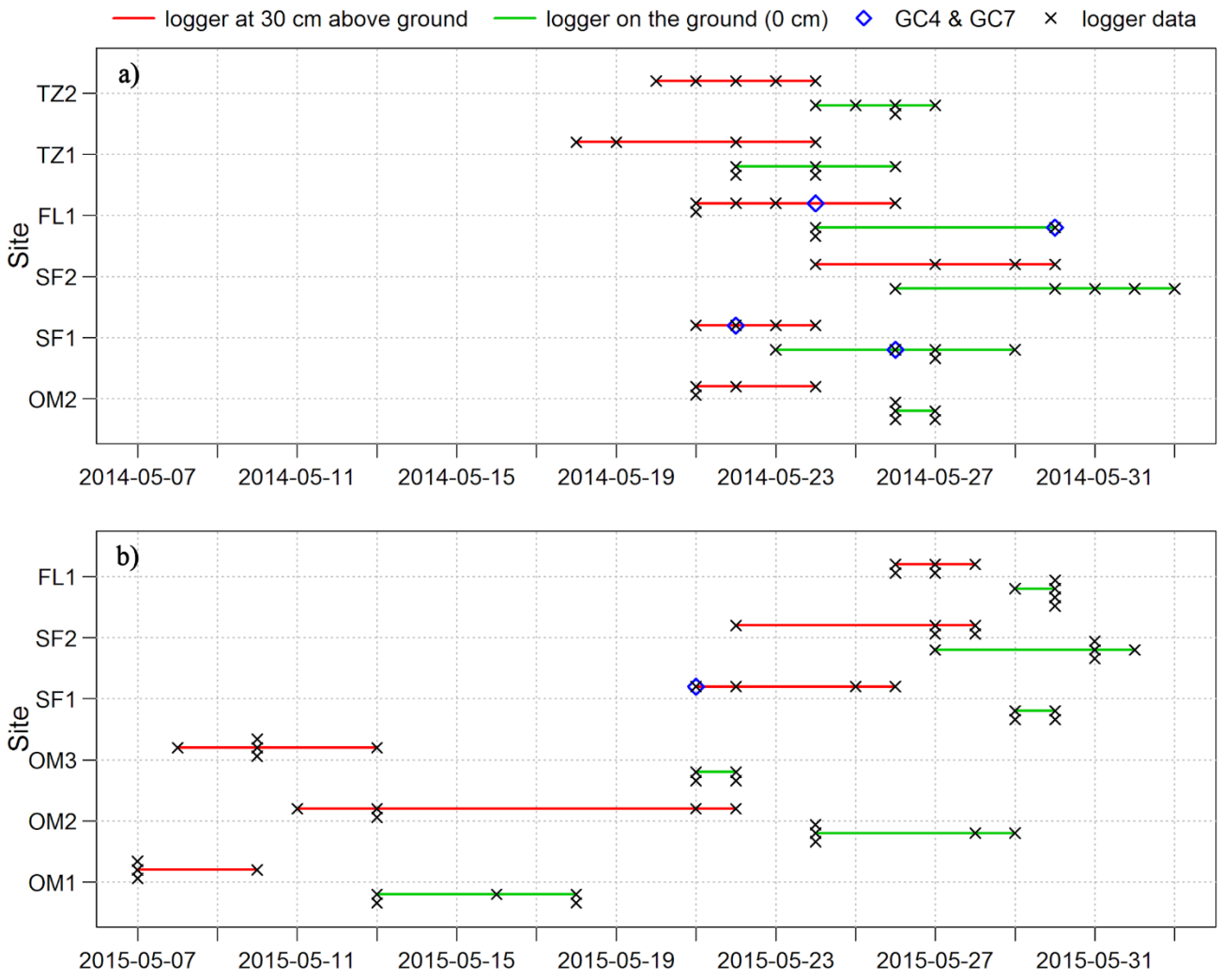

Figure 5. Observed variability in snow cover depletion in a) 2014 and b) 2015 for each test plot, derived from the logger temperatures. Each logger revealed at 30 cm above ground (red line) and on the ground (green line) is marked with "x". The loggers had technical problems at plots where only three or four measurements are shown. Reference measurements in the proximity of SF1 and FL1 are marked with blue diamonds. In 2015 there is only one blue diamond because data was not available after 25 May.

3.2 Melt rates and degree-day factors

Degree-day factors calculated for each site from temperature logger data were within the range reported in the literature (DeWalle and Rango, 2008; Hock, 2003; Kuusisto, 1984) and showed considerable

variation (Table 3, Figure 6). This was expected based on the variation observed in the measured data on snow properties, topography, vegetation and accuracy of determination of snowmelt dates. Median ddf for 2014 was 3.54 mm d^{-1} $°C^{-1}$ and for 2015 2.42 mm d^{-1} $°C^{-1}$, with a coefficient of variation (CV) of 0.37 and 0.24, respectively. The variation in ddf between the years is probably due to differences in global radiation amounts, which were 25% higher in May 2014, whereas cloudiness was higher in May 2015 (average 5/8) than in May 2014 (average 4/8).

The highest median ddf values for both study years were found in the highest elevation test plots (TZ1, TZ2 in 2014 and FL1 in 2015) on the south-facing slope (Table 3, Figure 6), which is in line with previous findings (e.g. Hock, 2003). The median ddf value obtained for the open mire (OM2) in 2014 was higher than in forested plots (SF2, FL1), but lower than in open transitional slope plots (TZ1, TZ2). The results obtained for southwestern forested test plot SF1 during 2014 were unexpected, as the density of the forest was higher than in forest plot FL1 but the median ddf for SF1 was equally high as for transitional slopes. However, Kuusisto (1984) indicates that the variation in ddf can be high at lower canopy densities, even though an overall decreasing trend in ddf can be seen with increased canopy density. The median ddf values for the open mires (OM1, OM2 and OM3) during 2015 were in the same range as found for the spruce forest (SF1 and SF2), which can partly be explained by the low canopy density at forested sites.

The variation was exceptionally high in 2014 in test plots TZ1, TZ2 and SF2. Apart from natural variation, the following explanations for pronounced variability can apply: 1) Variable canopy coverage (0-20%) in TZ2 and its exposure to solar radiation at its south-facing location on the mountain top, 2) a small brook and hummocks and snapped trees next to the sensors where the highest ddf values in TZ1 and SF2 were recorded, and 3) impact on melt speed due to the sensors (cf. Filippa et al., 2014; Reusser

and Zehe, 2011) and 4) invalid snow density assumptions due to possible high variability in spring resulting from a major snowfall event (Fig. 4a).

The forest plots (median 2.6 mm d^{-1} $°C^{-1}$) had slightly higher melt rates than mire plots (median 2.3 mm d^{-1} $°C^{-1}$). At the forest line, the melt rate was highest (median 3.2 mm d^{-1} $°C^{-1}$) of all the test plots which were used in both years. The higher elevation plots at the transitional slopes were observed to have the highest ddf values (median 4.6 mm d^{-1} $°C^{-1}$) in 2014, while the lowest ddf (median 2.0 mm d^{-1} $°C^{-1}$) was observed for low elevation mire in 2015. However, the values overlapped for different physiographical and vegetation types, with clear differences between the datasets for 2013/14 and 2014/15, which makes the use of the terrain-specific ddf challenging in distributed snow modelling. Furthermore, one set of parameters is only a satisfactory representation of the snow processes in selected areas, i.e. the parameters can be dynamic (Okkonen and Kløve, 2010).

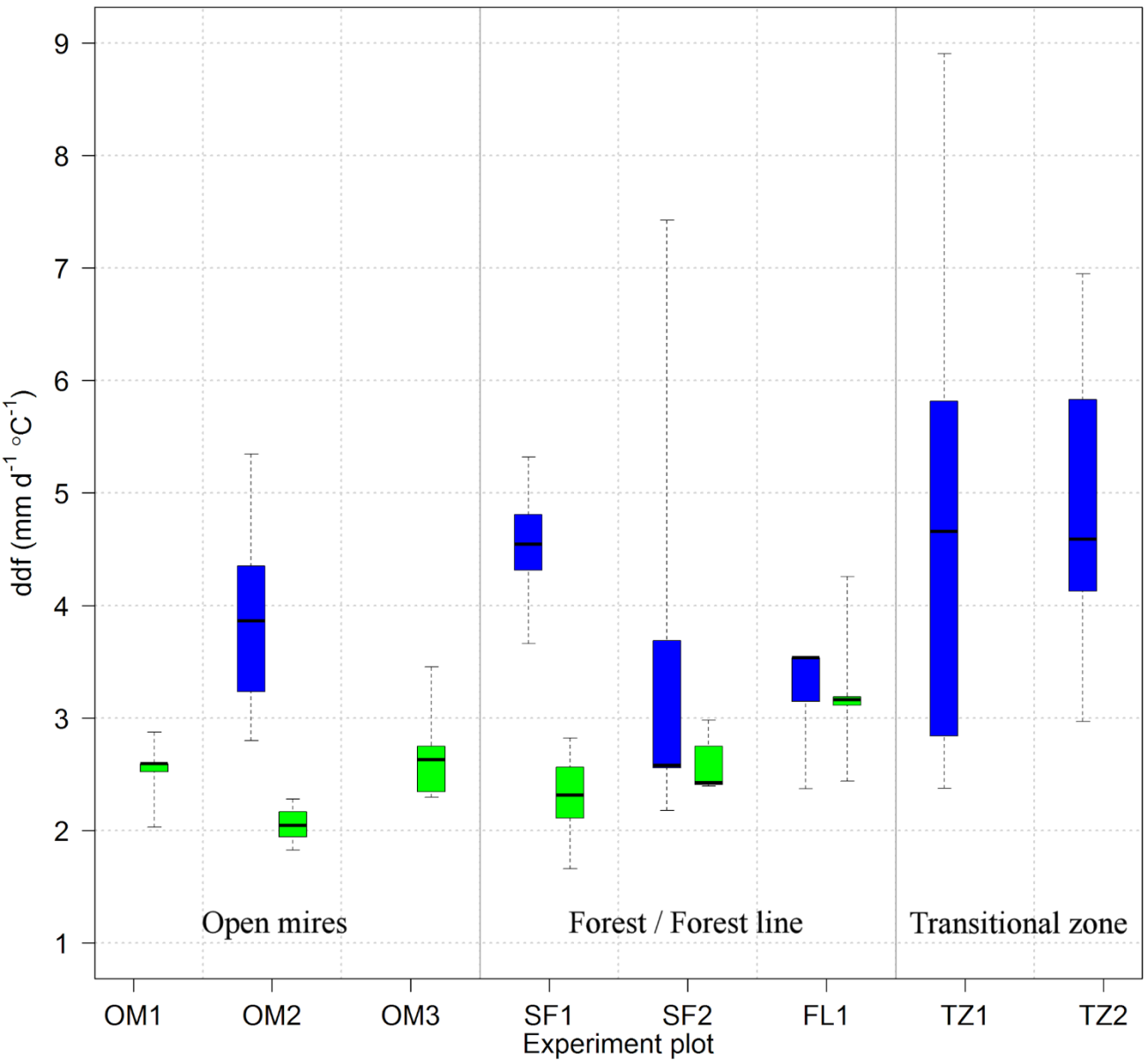

Figure 6. Boxplot of variation in calculated degree-day factors (ddf) at test plots in 2014 (blue) and 2015 (green). The boxes show the median, first and third quartiles of the data, while the whiskers show the minimum and maximum values.

Table 3. Calculated degree-day factor (ddf, mm d^{-1} °C^{-1}) for each test point, plot and whole experimental area during 2014[1] and 2015[1]. Vegetation: open mire (orange), forest/forest line (green), transitional zone (yellow).

	1	2	3	4	5	Mean	Median
OM1	-/2.87	-/2.03	-/NA	-/2.59	-/2.59	-/2.52	-/2.59
OM2	2.80/2.04	5.35/1.84	4.35/2.28	NA/1.83	3.23/2.28	3.93/2.05	3.79/2.04
OM3	-/NA	-/2.75	-/2.29	-/3.45	-/2.34	-/2.71	-/2.55
SF1	3.66/2.11	4.81/1.66	4.31/NA	NA/2.82	5.32/2.56	4.53/2.29	4.56/2.34
SF2	2.56/2.39	2.59/2.42	2.18/2.88	NA/2.39	7.43[3]/2.98	3.69/2.61	2.57/2.42
FL1	3.54/3.16	NA/3.16	2.37/2.44	3.53/3.06	NA/4.25	3.14/3.21	3.54/3.16
TZ1	2.84/-	5.82/-	8.91[2]/-	2.38/-	NA/-	4.98/-	4.33/-
TZ2	6.95/-	3.67/-	6.69/-	4.59/-	2.97/-	4.97/-	4.59/-
ALL	-	-	-	-	-	4.28/2.57	3.66/2.44

[1]First value is from 2014 and second from 2015.

[2]Small brook observed at the logger location when fetching the loggers.

[3]Hummock and snapped trees observed at the logger location when fetching the loggers.

3.3 Testing of melting rates using a degree-day model

With relatively simple field measurements and a snow model (Appendix A), it was possible to calculate ddf and simulate snow accumulation, melt timing and rate. The model performed relatively well, as can be seen in the example for test plot SF1 for both winters (Figs. 7 and 8). In addition to calculated and scaled ddfs in melt equation (A.4), determined separately for the winters 2013/2014 and 2014/2015, only

the correction factor for snowfall (CF_s) was recalibrated for winter 2014/2015. The CF_s values were almost the same for both winters (1.07 at SF1.5 in 2014 and 1.06 at SF1.2 in 2015, while averages of all five values at SF1 were 1.00 in 2014 and 1.01 in 2015), which suggests that SWE field measurements would not be needed after the first year of measurement. Estimated runoff timing agreed relatively well with the increase in soil moisture (Figs. 7 and 8).

3.3.1 Critical moment for snowmelt initiation

Calculated ddf at SF1.5 (2014) and SF1.2 (2015), the empirical snow model and soil moisture content at 20 cm below ground at the adjacent reference measurement station GC7 were used to analyse the critical moment when the snowpack started to generate outflow (Figs. 7 and 8). Modelled melt water outflow from the snowpack in 2014 started in mid-April (Fig. 7), which was indicated by increasing soil moisture content (SMC) a few days after a warm spell. Modelled melt periods after the initial start of the snowpack outflow were also evident from the soil moisture level, which reached its maximum during the final phase of the modelled melt, approximately after the third week in May. The SMC value close to maximum was maintained for 3-5 days after all snow had melted at the test point. A 3-4 day delay was observed between the start of the model outflow and an increase in soil water content 20 cm below the ground. The possible error in the magnitude of daily outflow was difficult to estimate using available data. Snow pillow, lysimeter or similar measuring equipment would be needed for such analysis.

The temperature data from the loggers on the ground and 30 cm above the ground alone were not sufficient to estimate the time when the snowpack outflow was initiated and observed data on SWE were needed. Interestingly, the date of measurement of the observed data did not seem to have a major impact on the modelling results, although many previous studies suggest that the measurements should be made during maximum SWE (Anderton et al., 2002; Clark et al., 2011; Kuusisto, 1984). Lundquist and Lott

(2008) avoided the need for calibration by assuming that the melt rate is constant and used a reverse SWE reconstruction method (e.g. Durand et al., 2008) from the snow disappearance date to the maximum SWE at a point. In our study, the maximum SWE and date of snow cover depletion were not correlated for winter 2013/2014, but there was a significant correlation ($\tau = 0.55$, $p<0.001$, $n = 28$) between SWE measured in the middle of the snow accumulation season and snow cover depletion date in winter 2014/2015. Reusser and Zehe (2011) used nine sensors with 15 cm spacing for snow depth and cold content estimation. Their approach provides more information on the temperature profile at a point and thus the moment when the cold content is zero can be estimated without additional calibration measurements. The downside of their method for modelling purposes is that SWE needs to be estimated without calibration measurements and that point measurements provide no information about micro-/local scale variation in the snow cover.

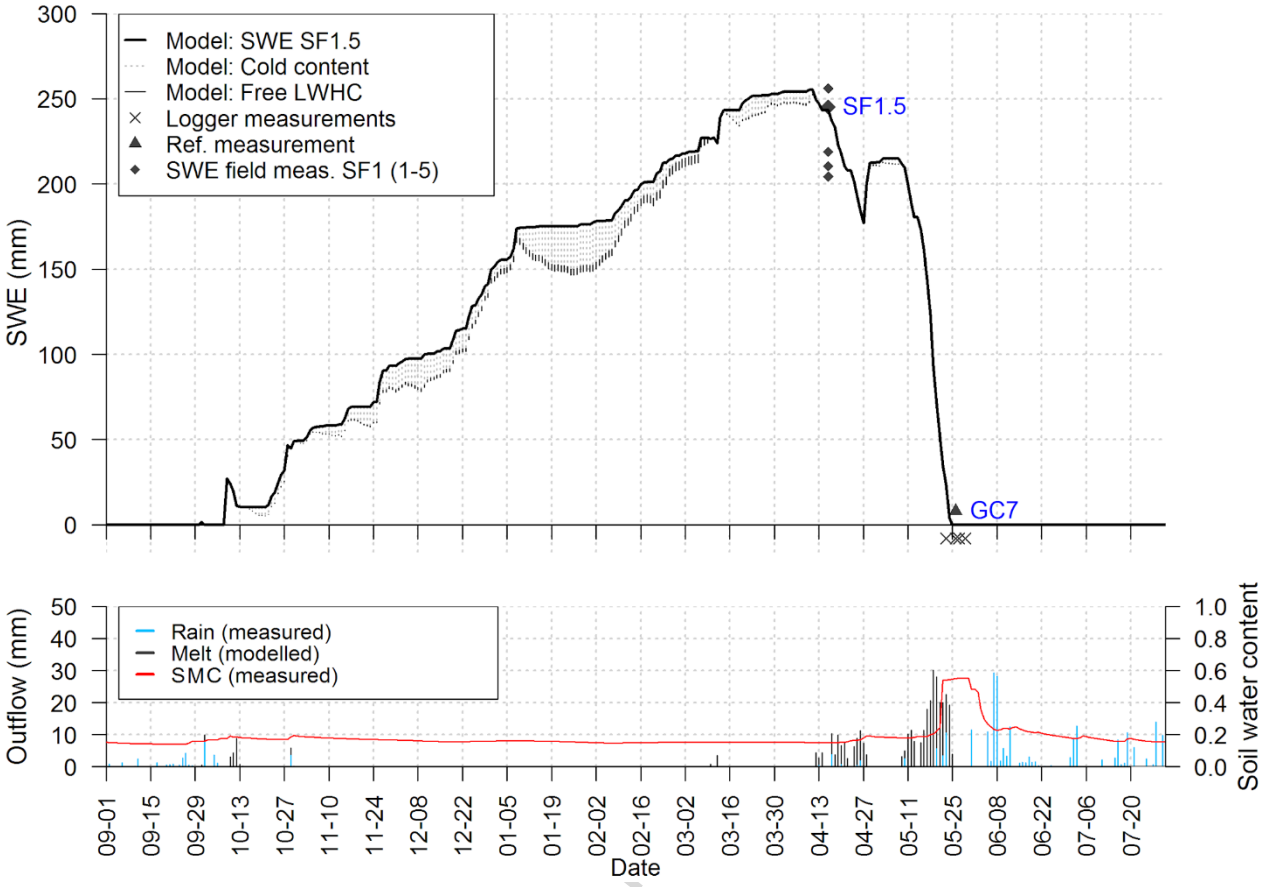

Figure 7. Upper graph: Modelled snow water equivalent (SWE) (black), cold content, representing the required refrozen liquid water equivalent to heat the snowpack to 0 °C (dashed light grey) and free liquid water holding capacity (LWHC), representing the free liquid water holding capacity in the snowpack (dark grey) at SF1.5. Measured SWE at all five test points in plot SF1 (dark grey) on 16 April 2014. Depletion date for snow cover at GTK GC7 reference site (grey triangle) and at SF1 test points (grey crosses). Lower graph: Modelled outflow from the snowpack as melt snow (dark grey) and measured rain (light blue) at SF1.5. Soil water content measured 20 cm below ground at GTK GC7 (red).

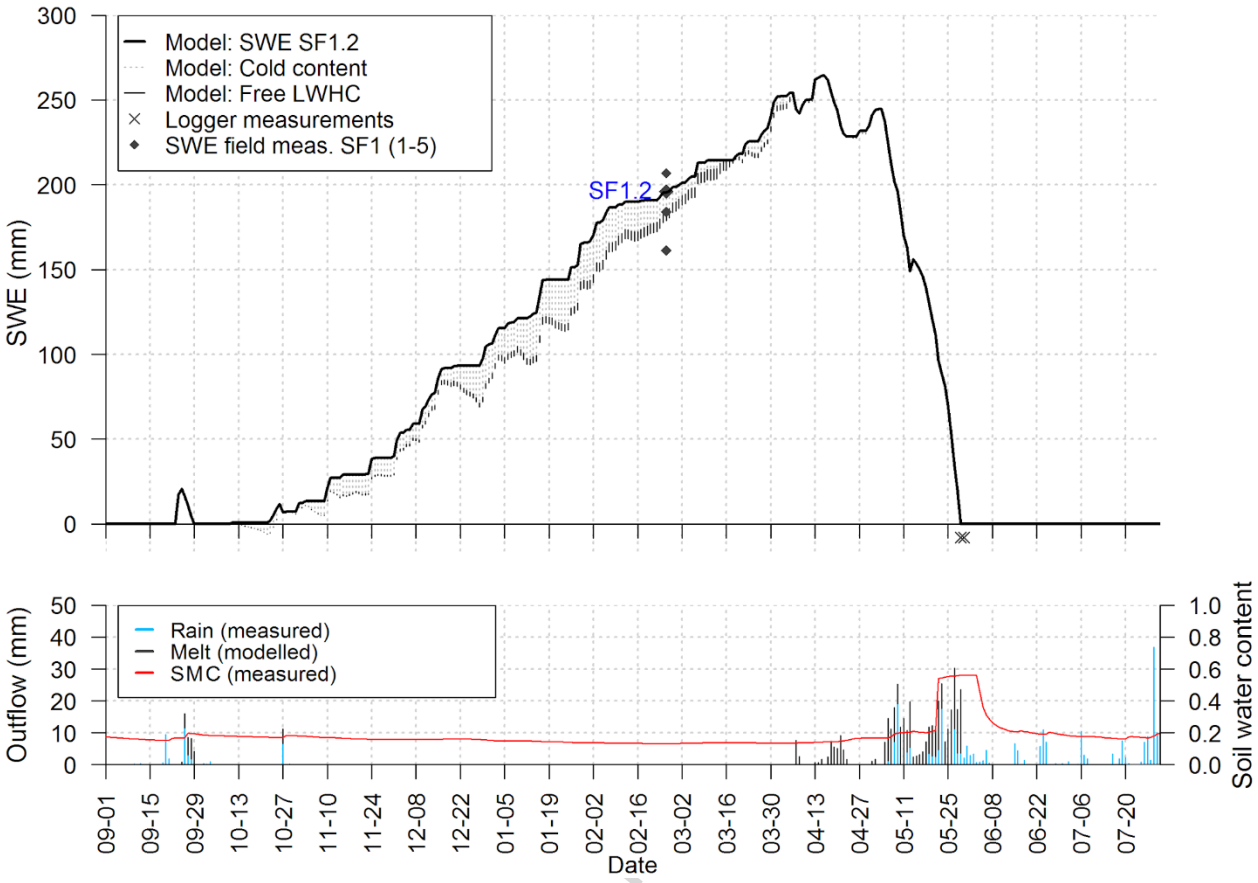

Figure 8. Upper graph: Modelled snow water equivalent (SWE) (black), cold content, representing the required refrozen liquid water equivalent to heat the snowpack to 0 °C (dashed light grey) and free liquid water holding capacity (LWHC), representing the free liquid water holding capacity in the snowpack (dark grey) at SF1.2. Measured SWE at all five test points in plot SF1 (dark grey) on 25 February 2015. Depletion date for snow cover at SF1 test points (grey crosses). Lower graph: Modelled outflow from the snowpack as melt snow (dark grey) and rain (light blue) at SF1.2. Soil water content measured 20 cm below ground at GTK GC7 (red).

3.3.2 Spatial variation in snowmelt at study area

The snow model developed was run for all sites using calculated ddfs for each study point and median annual ddfs for the whole study area to analyse the performance of the estimated melt rates and the spatial

variation of the snowmelt. A wide range of SWE in the study area and higher abundance of snow compared with surrounding snow courses was observed (Figs. 9 and 10). The goodness of the fit between the model and measured SWE during logger installation was excellent (Nash-Sutcliffe efficiency 0.99), while bias was -2.04 mm in 2014 and 0.06 mm in 2015. Normally, the correction factor for snowfall is larger than 1, because precipitation gauges tend to underestimate snowfall, but here a wide spread of factors from 0.66 to 1.64 was used. The high natural variation in snow accumulation justified this large spread. However, the approach can lead to large errors in SWE under anomalous climate conditions. When using the snowfall correction method, we recommend at least one SWE measurement towards the end of the snow season.

The vast majority of the modelled snowmelt end dates were within the range of measured dates (Figs. 9 and 10), the median error being zero days in winter 2013/2014 and zero days in winter 2014/2015 (RMSE 3.28 and 3.79 days, respectively). The modelled melt was delayed in open areas or areas with low canopy coverage, whereas it was early in forested areas (Fig. 11). The delay was greatest for the open mire (OM1) at the lowest elevation in winter 2014/2015, where the snow cover was depleted first. However, for the open mire OM2 in winter 2013/2014, the median melt date was 0.5 days earlier than measured. The precision of the model varied between years, with predictions being most precise for transitional slope (TZ1) in 2013/2014 and forest plots (SF2) in 2014/2015. Open mires had a large spread during both years.

The model in which calculated point specific ddfs were used clearly outperformed the model in which the annual median of the calculated ddfs was used in 2013/2014 (RMSE 4.04 days), but in 2014/2015 (RMSE 3.80 days) the results were similar. This shows the benefit of the method, especially in years with high spatial variability of snow melt rates.

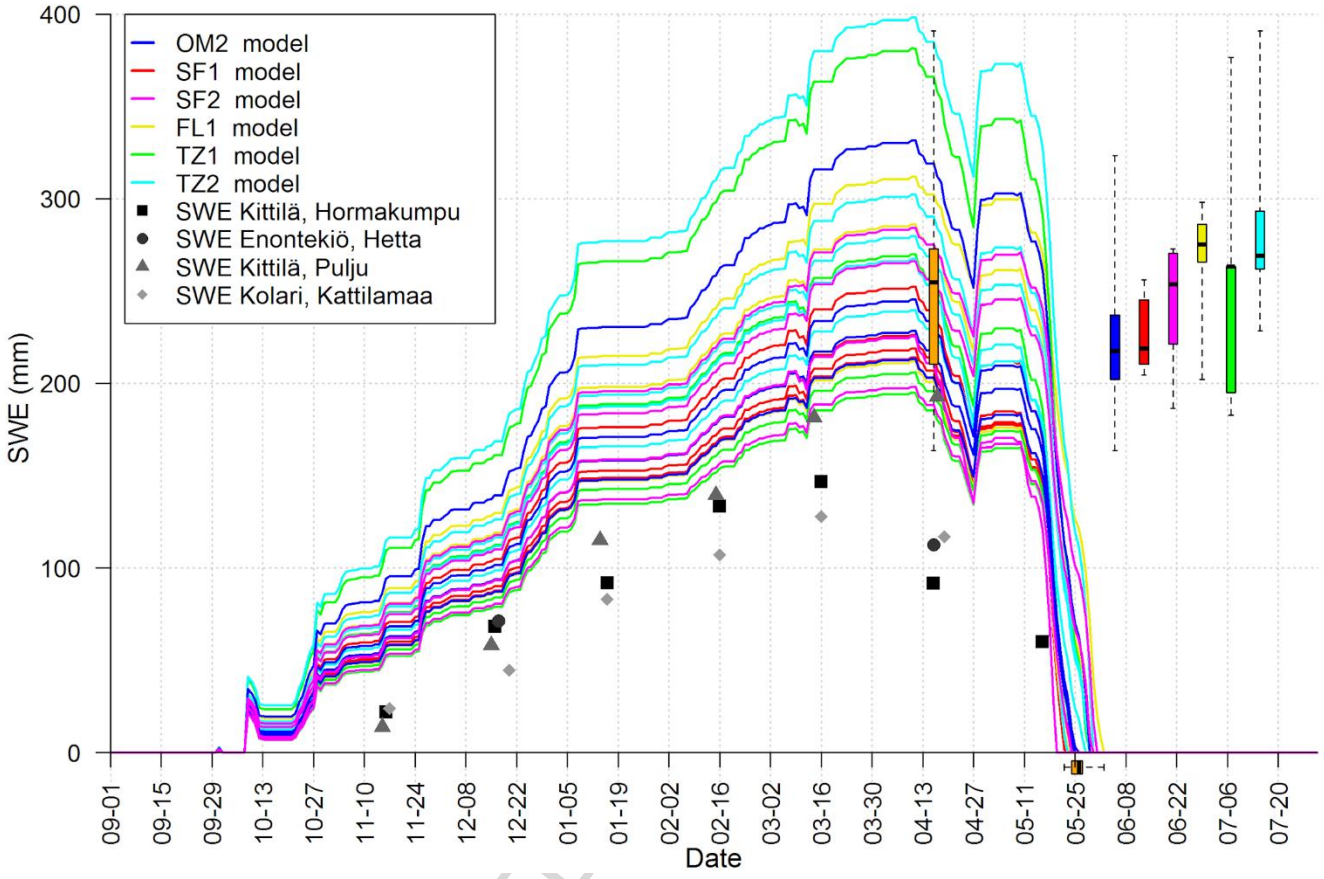

Figure 9. Modelled snow water equivalent (SWE) for each test point during 2013/2014. Measured SWE for each test plot is shown as vertical boxplots at the right side of the diagram. Combined measured SWE for all test points and measured dates for complete snowmelt determined using temperature loggers are shown in orange vertical and horizontal boxplots, respectively. Grayscale points (square, circle, triangle and diamond) show the snow course SWE measurement data closest to the study area in the region.

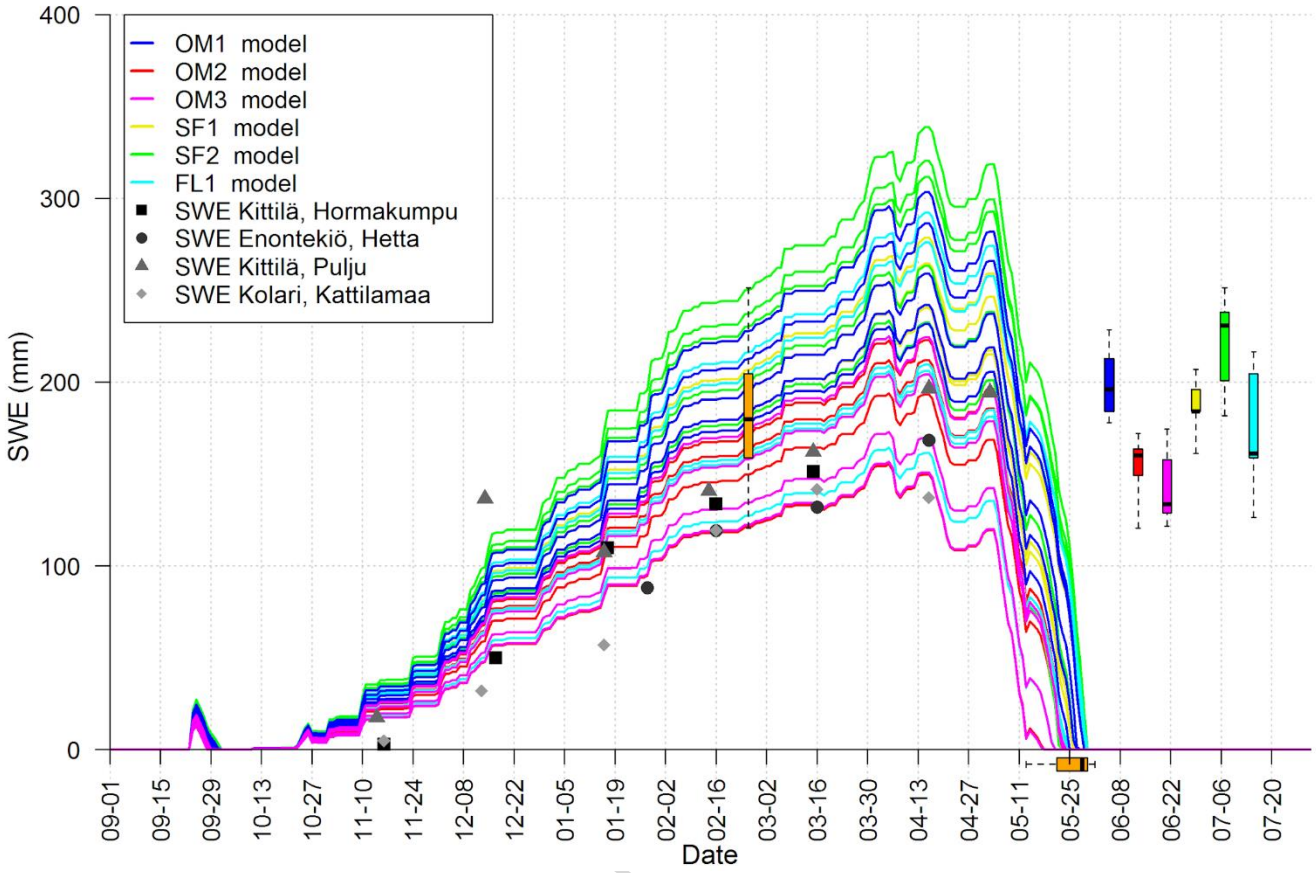

Figure 10. Modelled snow water equivalent (SWE) for each test point during 2014/2015. Measured SWE for each test plot is shown as vertical boxplots at the right side of the diagram. Combined measured SWE for all test points and measured dates for complete snowmelt determined using temperature loggers are shown in orange vertical and horizontal boxplots, respectively. Grayscale points (square, circle, triangle and diamond) show the snow course SWE measurement data closest to the study area in the region.

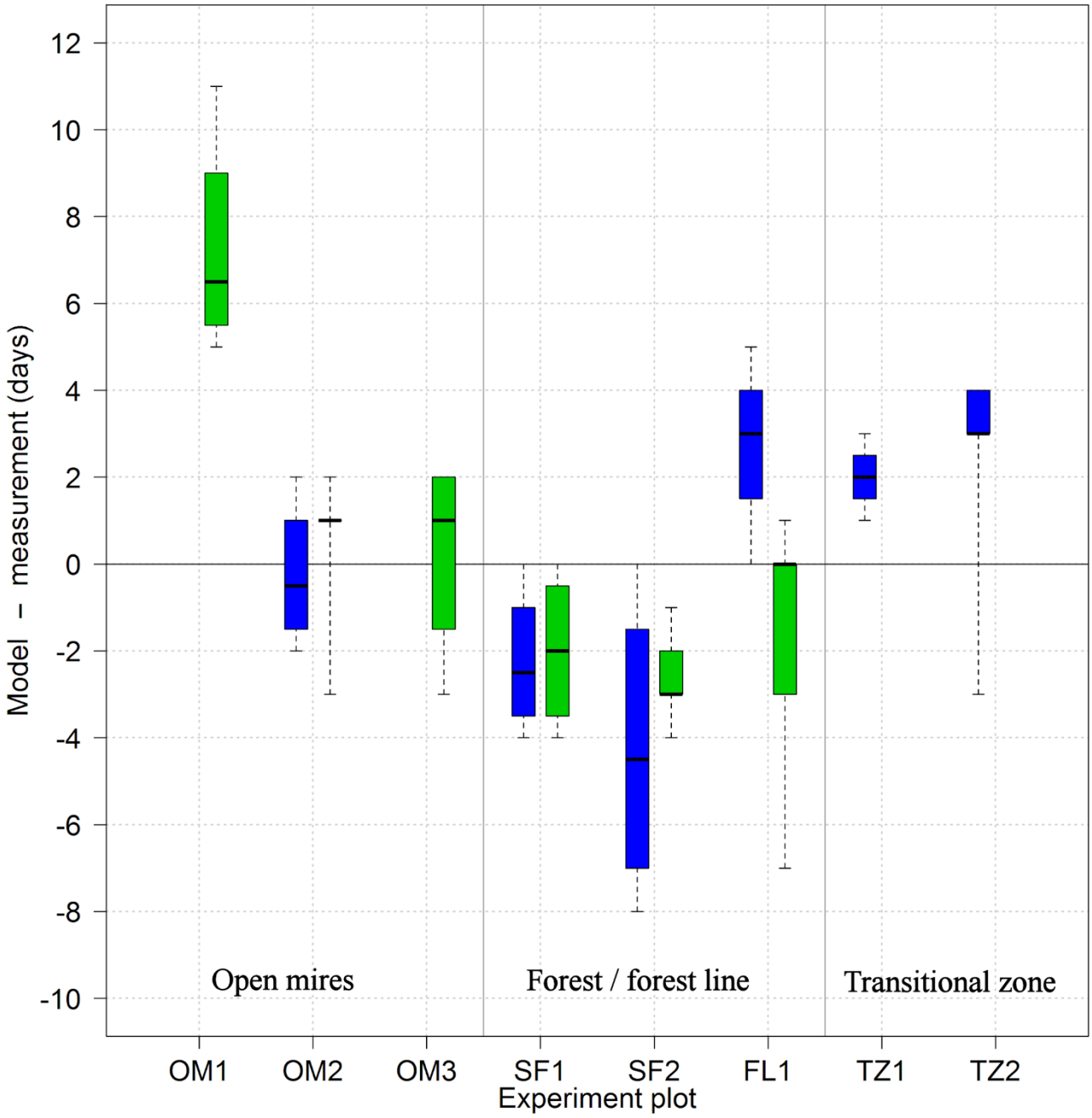

Figure 11. Difference between modelled and measured end of snow cover (date when all snow had melted) in spring 2014 (blue) and 2015 (green).

3.4 Usability of simple snow model and snow pack temperature monitoring in practice

The method developed in this study was found to be a cost-effective way of obtaining continuous data on the micro- and local-scale variation in snow cover depletion and snowmelt rates in different physiographical and vegetation conditions. The advantages over other low-cost methods, e.g. snow stakes and digital cameras, include information about the snow temperature, low power (electricity) requirements and robustness. Although snow pack temperature and snow melt patterns have been studied previously (Cunningham et al., 2006; Fujihara et al., 2017; Gottfried et al., 2002; Lundquist and Lott, 2008; Raleigh et al., 2013; Reusser and Zehe, 2011), we developed a new assessment method which can be used to estimate degree-day factor (ddf) and melt rates. More replicates and auxiliary data on snow accumulation and melt (SWE) would have been an advantage to better validate the developed measurement technique and to support more physically based snow modelling. However, considering the remoteness of the field site, we had unusually high quality automated measurements on snow depth and soil water content to validate our methodology. Moreover, the calculated date when the snow cover was completely depleted was used successfully in snow model calibration and the calculated ddf values used in model parameterisation decreased the need for calibration.

In future applications using wireless connections, the temperature loggers could be used to obtain real-time information on the snowpack for operational use and assimilating up-to-date data on snow cover for distributed hydrological modelling. Furthermore, the method can be used to determine the spatiotemporal distribution of SWE, which is essential for deriving snow depletion curves (Luce et al., 1999; Saloranta, 2014; Winstral and Marks, 2014). Lundquist and Lott (2008) suggest that for a 100-m grid cell, approximately 5-10 sensors are needed to capture the mean SWE values of the grid cell with accuracy of ±20% and CV within accuracy of ±0.2. Our method could also be used for long-term snow measurements, for example to support snow course measurements and/or to provide the ground truth in

remote sensing, by establishing fixed measurement stations. This could extend the representativeness of spatial distribution of the snow cover to include areas where current measurements are not representative and to provide real-time information about the snow cover when wireless sensors are included. Because of the relatively low resource requirement of our new method, it also has potential for use in short-term measurement campaigns in previously ungauged regions or areas where the current measurement network is too sparse.

4. Conclusions

This study showed that low-cost temperature loggers are a feasible way of obtaining high-resolution temperature data which, together with the algorithm developed, can be used to measure spatiotemporal variations in snowmelt rates. The results indicated that snow ablation occurred earlier in open mires (peatland), transitional slopes and areas with low canopy density than in forested plots (Fig. 5). Furthermore, the calculated degree-day factor values were suggested to be higher in open and sparsely forested areas at higher elevations, whereas mires and forested plots had lower values, especially in latter study period. However, it is difficult to determine the typical behaviour of degree-day factors for different vegetation types because of apparent differences between our study years. The method was able to reveal high micro- and local-scale and inter-annual variation in snowmelt rates, which provides novel field evidence to highlight the well-known problems in using static degree-day factor values in operative snowmelt models.

We successfully demonstrated that the logger data can be used in model calibration and melt rate parameterisation using a simple snow model, with clear improvement in results compared with lumped degree day factor. The results show that the method has the potential to reduce the calibration needed in degree-day snow models. Moreover, the method can be used to support on-going snow measurements

by increasing the spatial representativeness of data on variations in snow cover. It has also the potential to be used to determine the snow depletion curves and sub-grid snow variability in distributed snow models and as the first tool for measuring snowpack variations in previously ungauged or remote basins. The method could be further improved by adding more sensors horizontally in the snow column and using snow density reference measurements for each test plot. The procedure and method could be applied to stationary measurement stations with fixed logger positions and wireless connectivity to acquire data for real-time operational use.

Acknowledgements

This study was funded by the Maa- ja vesitekniikan tuki ry. We gratefully acknowledge the help of staff and trainees at the Water Resources and Environmental Engineering Research Unit, University of Oulu, Finland. We also would like to thank the Finnish Meteorological Institute and Finnish Environmental Institute for providing the weather and snow course data. The topographical data were sourced from the National Land Survey of Finland open database.

References

Anderson, E.A., 1973. National Weather Service River Forecast System- Snow Accumulation and Ablation Model, NOAA Technical Memorandum NWS HYDRO-17. US Department of Commerce, NOAA, NWS.

Anderton, S.., White, S.., Alvera, B., 2002. Micro-scale spatial variability and the timing of snow melt runoff in a high mountain catchment. J. Hydrol. 268, 158–176. doi:10.1016/S0022-1694(02)00179-8

Bair, E.H., Rittger, K., Davis, R.E., Painter, T.H., Dozier, J., 2016. Validating reconstruction of snow water equivalent in California's Sierra Nevada using measurements from the NASAAirborne Snow

Observatory. Water Resour. Res. 52, 8437–8460. doi:10.1002/2016WR018704

Barnett, T.P., Adam, J.C., Lettenmaier, D.P., 2005. Potential impacts of a warming climate on water availability in snow-dominated regions. Nature 438, 303–309. doi:10.1038/nature04141

Bokhorst, S., Pedersen, S.H., Brucker, L., Anisimov, O., Bjerke, J.W., Brown, R.D., Ehrich, D., Essery, R.L.H., Heilig, A., Ingvander, S., Johansson, C., Johansson, M., Jónsdóttir, I.S., Inga, N., Luojus, K., Macelloni, G., Mariash, H., McLennan, D., Rosqvist, G.N., Sato, A., Savela, H., Schneebeli, M., Sokolov, A., Sokratov, S.A., Terzago, S., Vikhamar-Schuler, D., Williamson, S., Qiu, Y., Callaghan, T. V., 2016. Changing Arctic snow cover: A review of recent developments and assessment of future needs for observations, modelling, and impacts. Ambio 45, 516–537. doi:10.1007/s13280-016-0770-0

Bormann, K.J., Westra, S., Evans, J.P., McCabe, M.F., 2013. Spatial and temporal variability in seasonal snow density. J. Hydrol. 484, 63–73. doi:10.1016/j.jhydrol.2013.01.032

Bühler, Y., Marty, M., Egli, L., Veitinger, J., Jonas, T., Thee, P., Ginzler, C., 2015. Snow depth mapping in high-alpine catchments using digital photogrammetry. Cryosph. 9, 229–243. doi:10.5194/tc-9-229-2015

Campell Scientific, 2016. Instruction Manual: SR50A, SR50A-316SS, and SR50AH Sonic Ranging Sensors [WWW Document]. URL http://s.campbellsci.com/documents/us/manuals/sr50a.pdf (accessed 11.10.16).

Clark, M.P., Hendrikx, J., Slater, A.G., Kavetski, D., Anderson, B., Cullen, N.J., Kerr, T., Örn Hreinsson, E., Woods, R.A., 2011. Representing spatial variability of snow water equivalent in hydrologic and land-surface models: A review. Water Resour. Res. 47, n/a-n/a. doi:10.1029/2011WR010745

Cohen, J., Lemmetyinen, J., Pulliainen, J., Heinila, K., Montomoli, F., Seppanen, J., Hallikainen, M.T., 2015. The Effect of Boreal Forest Canopy in Satellite Snow Mapping - A Multisensor Analysis. IEEE Trans. Geosci. Remote Sens. 53, 6593–6607. doi:10.1109/TGRS.2015.2444422

Cunningham, C., Zimmermann, N.E., Stoeckli, V., Bugmann, H., 2006. Growth response of Norway spruce saplings in two forest gaps in the Swiss Alps to artificial browsing, infection with black snow mold, and competition by ground vegetation. Can. J. For. Res. 36, 2782–2793. doi:10.1139/x06-156

De Michele, C., Avanzi, F., Passoni, D., Barzaghi, R., Pinto, L., Dosso, P., Ghezzi, A., Gianatti, R., Vedova, G. Della, 2016. Using a fixed-wing UAS to map snow depth distribution: An evaluation at peak accumulation. Cryosphere 10, 511–522. doi:10.5194/tc-10-511-2016

DeWalle, D.R., Rango, A., 2008. Principles of Snow Hydrology. Cambridge University Press, Cambridge, United Kindom.

Durand, M., Molotch, N.P., Margulis, S.A., 2008. A Bayesian approach to snow water equivalent reconstruction. J. Geophys. Res. 113, 1–15. doi:10.1029/2008JD009894

Filippa, G., Maggioni, M., Zanini, E., Freppaz, M., 2014. Analysis of continuous snow temperature profiles from automatic weather stations in Aosta Valley (NW Italy): Uncertainties and applications. Cold Reg. Sci. Technol. 104–105, 54–62. doi:10.1016/j.coldregions.2014.04.008

FMI, 2016. Talvitilastot [WWW Document]. URL http://ilmatieteenlaitos.fi/talvitilastot (accessed 11.10.16).

FMI, 2015. Snow statistics [WWW Document]. URL http://en.ilmatieteenlaitos.fi/snow-statistics (accessed 11.10.16).

Fujihara, Y., Takase, K., Chono, S., Ichion, E., Ogura, A., Tanaka, K., 2017. Influence of topography and forest characteristics on snow distributions in a forested catchment. J. Hydrol. 546, 289–298. doi:10.1016/j.jhydrol.2017.01.021

Gelfan, A.N., Pomeroy, J.W., Kuchment, L.S., 2004. Modeling Forest Cover Influences on Snow Accumulation, Sublimation, and Melt. J. Hydrometeorol. 5, 785–803. doi:10.1175/1525-7541(2004)005<0785:MFCIOS>2.0.CO;2

Gottfried, M., Pauli, H., Reiter, K., Grabherr, G., 2002. Potential Effects of CLimate Change on Alpine and Nival Plants in the Alps, in: Körner, C., Spehn, E.M. (Eds.), Mountain Biodiversity: A Global Assessment. The Parthenon Publishing Group, London, pp. 213–223.

Gray, D.M. et al., 1978. Snow Accumulation and Distribution, Modeling Snow Cover Runoff. Hanover, New Hampshire, 26-29 September, 1978.

He, M., Hogue, T.S., Franz, K.J., Margulis, S.A., Vrugt, J.A., 2011. Characterizing parameter sensitivity and uncertainty for a snow model across hydroclimatic regimes. Adv. Water Resour. 34, 114–127. doi:10.1016/j.advwatres.2010.10.002

Hock, R., 2003. Temperature index melt modelling in mountain areas. J. Hydrol. 282, 104–115. doi:10.1016/S0022-1694(03)00257-9

IPCC, 2014. Climate Change 2014: Impacts, Adaptation, and Vulnerability. Part B: Regional Aspects. Contribution of Working Group II to the Fifth Assessment Report of the Intergovernmental Panel on Climate Change [Barros, V.R., C.B. Field, D.J. Dokken, M.D. Mastrandre. Cambridge University Press, Cambridge, United Kingdom and New York, NY, USA.

Irannezhad, M., Ronkanen, A.K., Kløve, B., 2016. Wintertime climate factors controlling snow resource decline in Finland. Int. J. Climatol. 36, 110–131. doi:10.1002/joc.4332

Jost, G., Weiler, M., Gluns, D.R., Alila, Y., 2007. The influence of forest and topography on snow accumulation and melt at the watershed-scale. J. Hydrol. 347, 101–115. doi:10.1016/j.jhydrol.2007.09.006

Kinar, N.J., Pomeroy, J.W., 2015. Measurement of the physical properties of the snowpack. Rev. Geophys. 53, 481–544. doi:10.1002/2015RG000481

Kokkonen, T.S., Jakeman, A.J., 2001. A comparison of metric and conceptual approaches in rainfall-runoff modeling and its implications. Water Resour. Res. 37, 2345–2352. doi:10.1029/2001WR000299

Korhonen, L., Heikkinen, J., 2009. Automated analysis of in situ canopy images for the estimation of forest canopy cover. For. Sci. 55, 323–334.

Koskinen, J.T., Pulliainen, J.T., Hallikainen, M.T., 1997. The use of ers-1 sar data in snow melt monitoring. IEEE Trans. Geosci. Remote Sens. 35, 601–610. doi:10.1109/36.581975

Krause, P., Boyle, D.P., Bäse, F., 2005. Comparison of different efficiency criteria for hydrological model assessment. Adv. Geosci. 5, 89–97. doi:10.5194/adgeo-5-89-2005

Kumar, S., Zwiers, F., Dirmeyer, P.A., Lawrence, D.M., Shrestha, R., Werner, A.T., 2016. Terrestrial contribution to the heterogeneity in hydrological changes under global warming. Water Resour. Res. 52, 3127–3142. doi:10.1002/2016WR018607

Kuusisto, E., 1984. Snow accumulation and snowmelt in Finland, Publications of the Water Research Institute 55. National Board of Waters, Helsinki.

Legates, D.R., McCabe Jr., G.J., 1999. Evaluating the Use of "Goodness of Fit" Measures in Hydrologic and Hydroclimatic Model Validation. Water Resour. Res. 35, 233–241. doi:10.1029/1998WR900018

Leinss, S., Wiesmann, A., Lemmetyinen, J., Hajnsek, I., 2015. Snow Water Equivalent of Dry Snow Measured by Differential Interferometry. IEEE J. Sel. Top. Appl. Earth Obs. Remote Sens. 8, 3773–3790. doi:10.1109/JSTARS.2015.2432031

Link, T.E., Marks, D., 1999. Point simulation of seasonal snow cover dynamics beneath boreal forest canopies. J. Geophys. Res. Atmos. 104, 27841–27857. doi:10.1029/1998JD200121

Liston, G., Sturm, M., 1998. A snow-transport model for complex terrain. J. Glaciol. 44, 498–516.

Liston, G.E., 2004. Representing Subgrid Snow Cover Heterogeneities in Regional and Global Models. J. Clim. 17, 1381–1397. doi:10.1175/1520-0442(2004)017<1381:RSSCHI>2.0.CO;2

Liston, G.E., 1999. Interrelationships among Snow Distribution, Snowmelt, and Snow Cover Depletion: Implications for Atmospheric, Hydrologic, and Ecologic Modeling. J. Appl. Meteorol. 38, 1474–

1487. doi:10.1175/1520-0450(1999)038<1474:IASDSA>2.0.CO;2

Luce, C.H., Tarboton, D.G., Cooley, K.R., 1999. Sub-grid parameterization of snow distribution for an energy and mass balance snow cover model. Hydrol. Process. 13, 1921–1933. doi:10.1002/(SICI)1099-1085(199909)13:12/13<1921::AID-HYP867>3.0.CO;2-S

Lundberg, A., Granlund, N., Gustafsson, D., 2010. Towards automated "Ground truth" snow measurements-a review of operational and new measurement methods for Sweden, Norway, and Finland. Hydrol. Process. 24, n/a-n/a. doi:10.1002/hyp.7658

Lundquist, J.D., Lott, F., 2008. Using inexpensive temperature sensors to monitor the duration and heterogeneity of snow-covered areas. Water Resour. Res. 44, n/a-n/a. doi:10.1029/2008WR007035

Molotch, N.P., Barnard, D.M., Burns, S.P., Painter, T.H., 2016. Measuring spatiotemporal variation in snow optical grain size under a subalpine forest canopy using contact spectroscopy. Water Resour. Res. 52, 7513–7522. doi:10.1002/2016WR018954

Nolin, A.W., 2010. Recent advances in remote sensing of seasonal snow. J. Glaciol. 56, 1141–1150. doi:10.3189/002214311796406077

Ohmura, A., 2001. Physical Basis for the Temperature-Based Melt-Index Method. J. Appl. Meteorol. 40, 753–761. doi:10.1175/1520-0450(2001)040<0753:PBFTTB>2.0.CO;2

Okkonen, J., Kløve, B., 2011. A sequential modelling approach to assess groundwater-surface water resources in a snow dominated region of Finland. J. Hydrol. 411, 91–107. doi:10.1016/j.jhydrol.2011.09.038

Okkonen, J., Kløve, B., 2010. A conceptual and statistical approach for the analysis of climate impact on ground water table fluctuation patterns in cold conditions. J. Hydrol. 388, 1–12. doi:10.1016/j.jhydrol.2010.02.015

Onset, 2015. HOBO Pedant Temperature Logger (UA-001-xx) Manual [WWW Document]. URL http://www.onsetcomp.com/files/manual_pdfs/9531-M MAN-UA-001.pdf (accessed 11.10.16).

Peel, M.C., Finlayson, B.L., McMahon, T.A., 2007. Updated world map of the Köppen-Geiger climate classification. Hydrol. Earth Syst. Sci. 11, 1633–1644. doi:10.5194/hess-11-1633-2007

Pirinen, P., Simola, H., Aalto, J., Kaukoranta, J.-P., Karlsson, P., Ruuhela, R., 2012. Climatological statistics of Finland 1981-2010, Reports 2012:1. Finnish Meteorological Institute, Helsinki.

Pomeroy, J.W., Gray, D.M., Hedstrom, N.R., Janowicz, J.R., 2002. Prediction of seasonal snow accumulation in cold climate forests. Hydrol. Process. 16, 3543–3558. doi:10.1002/hyp.1228

Raleigh, M.S., Rittger, K., Moore, C.E., Henn, B., Lutz, J.A., Lundquist, J.D., 2013. Ground-based testing of MODIS fractional snow cover in subalpine meadows and forests of the Sierra Nevada. Remote Sens. Environ. 128, 44–57. doi:10.1016/j.rse.2012.09.016

Rasmus, S., 2005. Snow pack structure characteristics in Finland - measurements and modelling. Rep. Ser. Geophys. No. 48. University of Helsinki.

Reusser, D.E., Zehe, E., 2011. Low-cost monitoring of snow height and thermal properties with inexpensive temperature sensors. Hydrol. Process. 25, 1841–1852. doi:10.1002/hyp.7937

Rice, R., Bales, R.C., 2010. Embedded-sensor network design for snow cover measurements around snow pillow and snow course sites in the Sierra Nevada of California. Water Resour. Res. 46, n/a-n/a. doi:10.1029/2008WR007318

Räisänen, J., Eklund, J., 2012. 21st Century changes in snow climate in Northern Europe: A high-resolution view from ENSEMBLES regional climate models. Clim. Dyn. 38, 2575–2591. doi:10.1007/s00382-011-1076-3

Saloranta, T., 2014. New version (v.1.1.1) of the seNorge snow model and snow maps for Norway. Norwegian Water Resources and Energy Directorate, Oslo, Norway.

Shook, K., Gray, D.M., 1996. Small-Scale Spatial Structure of Shallow Snowcovers. Hydrol. Process. 10, 1283–1292. doi:10.1002/(SICI)1099-1085(199610)10:10<1283::AID-HYP460>3.0.CO;2-M

Sturm, M., 2015. White water: Fifty years of snow research in WRR and the outlook for the future. Water

Resour. Res. 51, 4948–4965. doi:10.1002/2015WR017242

Sturm, M., Holmgren, J., Liston, G.E., 2009. Changes in snowpack and snowmelt runoff for key mountain regions. Hydrol. Process. 23, 78–94. doi:10.1002/hyp.7128

Sutinen, R., Hänninen, P., Venäläinen, A., 2008. Effect of mild winter events on soil water content beneath snowpack. Cold Reg. Sci. Technol. 51, 56–67. doi:10.1016/j.coldregions.2007.05.014

Sutinen, R., Närhi, P., Middleton, M., Hänninen, P., Timonen, M., Sutinen, M.L., 2012. Advance of Norway spruce (Picea abies) onto mafic Lommoltunturi fell in Finnish Lapland during the last 200 years. Boreas 41, 367–378. doi:10.1111/j.1502-3885.2011.00238.x

Sutinen, R., Äikää, O., Piekkari, M., Hänninen, P., 2009. Snowmelt infiltration through partially frozen soil in Finnish Lapland. Geophysica 45, 27–39.

Talbot, J., Plamondon, A.P., Lévesque, D., Aubé, D., Prévos, M., Chazalmartin, F., Gnocchini, M., 2006. Relating snow dynamics and balsam fir stand characteristics, Montmorency Forest, Quebec. Hydrol. Process. 20, 1187–1199. doi:10.1002/hyp.5938

Vajda, A., Venäläinen, A., Hänninen, P., Sutinen, R., 2006. Effect of vegetation on snow cover at the northern timberline: a case study in Finnish Lapland. Silva Fenn. 40, 195–207. doi:10.14214/sf.338

Vionnet, V., Brun, E., Morin, S., Boone, A., Faroux, S., Le Moigne, P., Martin, E., Willemet, J.M., 2012. The detailed snowpack scheme Crocus and its implementation in SURFEX v7.2. Geosci. Model Dev. 5, 773–791. doi:10.5194/gmd-5-773-2012

Winstral, A., Marks, D., 2014. Long-term snow distribution observations in a mountain catchment: Assessing variability, time stability, and the representativeness of an index site. Water Resour. Res. 50, 293–305. doi:10.1002/2012WR013038

Appendix A. The degree-day snow model

The snow model used in this study is based on the temperature index model described in DeWalle and Rango (2011). It simulates SWE, cold content, free liquid water-holding capacity and outflow from the snowpack for each time step (i), which was one day in this study. Inputs of the model are precipitation and temperature.

The precipitation input P_{i} (mm) is partitioned as snow $P_{s,\mathrm{i}}$ (mm) or rain $P_{r,\mathrm{i}}$ (mm) using a threshold temperature T_{crit} (°C) compared with air temperature $T_{a,i}$ (°C) (Eq. A.1 and A.2). Precipitation is corrected using a correction factor which can be set separately to snow CF_s (-) and rain CF_r (-) precipitation (Eqs. A.1 and A.2).

$$P_{s,i} = P_i \times CF_s, when\ T_{a,i} \leq T_{crit} \quad \text{(A.1)}$$

$$P_{r,i} = P_i \times CF_r, when\ T_{a,i} > T_{crit} \quad \text{(A.2)}$$

Snow water equivalent SWE_{i} (mm) (Eq. A.3) is increased during snowfall or when melt or rain water is stored in the snowpack, i.e. the liquid water-holding capacity $LWHC_i$ (mm) (Eq. A.7) is filled. Snow water equivalent SWE_{i} (Eq. A.3) is decreased and forms outflow O_{i} (mm) during snowmelt M_i (mm) and rain, but only after the cold content CC_{i} (mm) (Eq. A.5) is zero and liquid water storage $LWHC_i$ of the snowpack is full, i.e. liquid water is not refrozen or stored in the snowpack.

$$SWE_{\mathrm{i}+1} = SWE_{\mathrm{i}} + P_{i+1} - LWHC_{i+1} + LWHC_i - \left(M_{i+1} + P_{r,i+1}\right) \quad \text{(A.3)}$$

Snowmelt M_i (mm) (Eq. A.4) is calculated using the degree-day approach presented in DeWalle and Rango (2011). Degree-day factor $ddf_{temp,i}$ (mm °C^{-1} day^{-1}) was set to increase linearly from 1.0 (1 Sep) to calculated ddf (31 May) (A.4.1). The scaling for the calculated ddf was done because the measured degree-day factors represented the melt rates at the end of the melt season and they are known to increase towards the end of the snow season.

$$M_i = \begin{cases} ddf_{temp,i} \times \left(T_{a,i} - T_m\right), & \text{when } T_{a,i} \geq T_m \\ 0, & \text{when } T_{a,i} < T_m \end{cases} \quad \text{(A.4)}$$

$$ddf_{temp,i} = \begin{cases} 1.0, & \text{on 1 September} \\ b + \sqrt{ddf_{calc}}, & \text{on 31 May} \end{cases} \quad \text{(A.4.1)}$$

Cold content CC_{i} (mm) of the snowpack is calculated using an empirical degree-day cold-content model (Eq. A.5) (Anderson, 1973), using cold-content degree-day factor CCF (mm °C^{-1}) and the difference between snow surface T_s (°C) and air temperature.

$$CC_{\mathrm{i+1}} = CC_{\mathrm{i}} + CCF \times \left(T_{s,i+1} - T_{a,i+1}\right) \quad \text{(A.5)}$$

The snow surface temperature $T_{s,i}$ (°C) needed in the cold content model (Eq. A.5) is estimated using the temperature index method (Eq. A.6) (Anderson, 1973), with a dimensionless surface temperature factor TSF (-) and the difference between snow surface temperature at time step (i) and air temperature at time step (i+1).

$$T_{s,i+1} = T_{s,i} + TSF \times \left(T_{a,i+1} - T_{s,i}\right) \quad \text{(A.6)}$$

Liquid water-holding capacity $LWHC_i$ (mm) (Eq. A.7) of the snowpack is determined by multiplying the new snowfall by the maximum liquid water storage percentage of the snowpack f (%). The value represents the amount liquid water which can be held in snowpack against gravity and was selected to be 3 % (DeWalle and Rango, 2008; He et al., 2011), and it showed no sensitivity in initial model testing. Moreover, approximately equal values can be calculated using typical snowpack densities of ripe snowpack assuming liquid water-holding capacity to be 5 % of the total pore volume (Vionnet et al., 2012).

$$LWHC_{i+1} = LWHC_i + (f/100) \times P_{s,i+1} \quad \text{(A.7)}$$

When the model starts the calculations (i = 1) during a period when there is no snow, all the initial values can be set to zero, i.e. $SWE_{\mathrm{i}} = LWHC_i = CC_{\mathrm{i}} = T_{s,i} = O_i = 0$).

Set of parameters used in modelling is presented in table A1.

Table A1. Parameters used in the snow model, where they were used and how they were determined.

Parameter	Value	Determination method
Precipitation: form and snowfall correction		
$CF_{s(2013/2014)}$	0.77 – 1.64	Adjusted using SWE measurement
$CF_{s(2014/2015)}$	0.66 – 1.35	Adjusted using SWE measurement
T_{crit}	1.1 °C	Adjusted
Snow pack: melt		
T_m	−0.1 °C	Adjusted
$ddf_{temp,i}(1\ Sept)$	1.0 mm °C^{-1}	Adjusted
ddf_{calc}	2.18 – 8.91 mm °C^{-1} in 2014 and 1.66 – 4.25 mm °C^{-1} in 2015	Determined from logger data
b	0.72 for 2014 and 1.11 for 2015	Adjusted
Snow pack: cold content		
CCF	0.2 mm °C^{-1}	Fixed during initial model testing
TSF	0.1	Fixed during initial model testing
Snow pack: Liquid water holding capacity		
f	3 %	Fixed during initial model testing

Appendix B: Supplementary material

R-scripts: High resolution temperature data analyser, Snow model

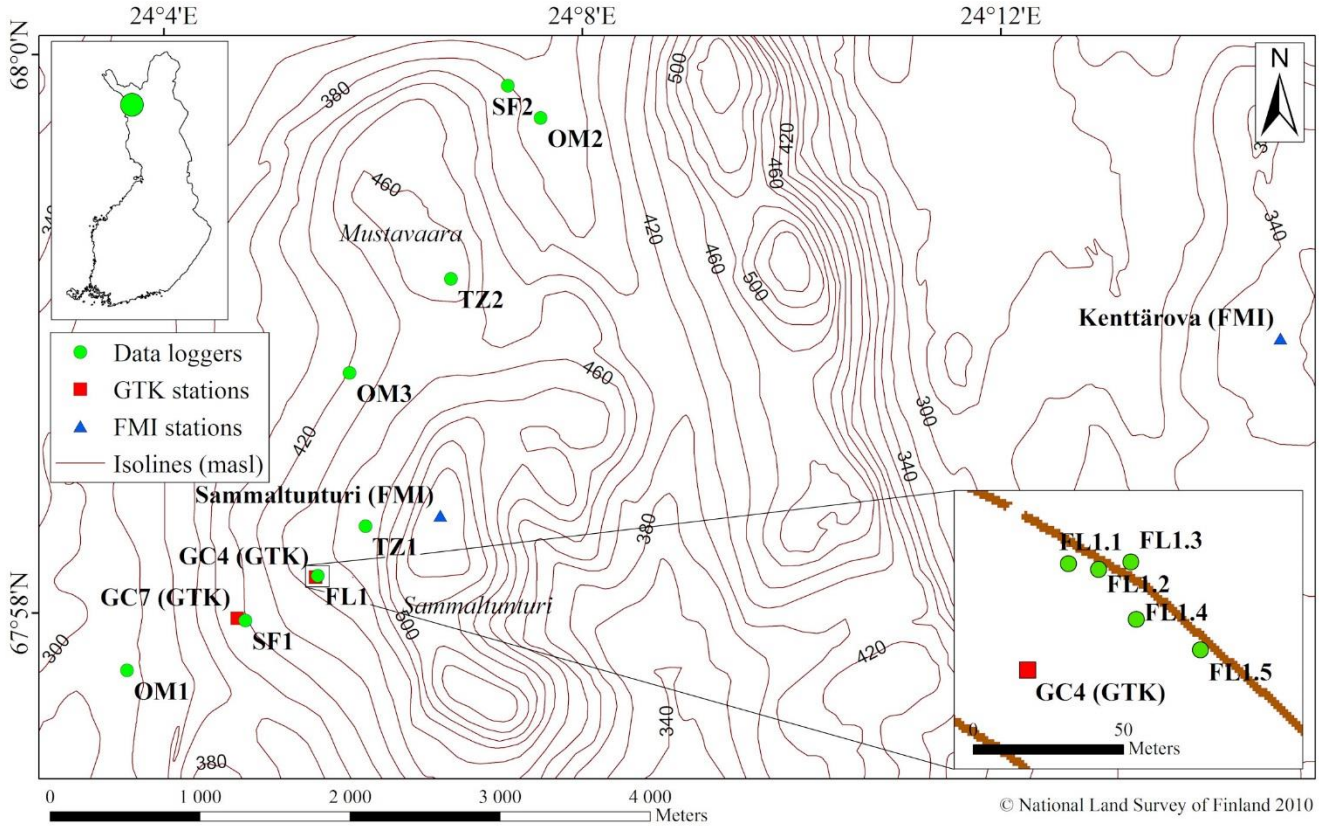


OM1

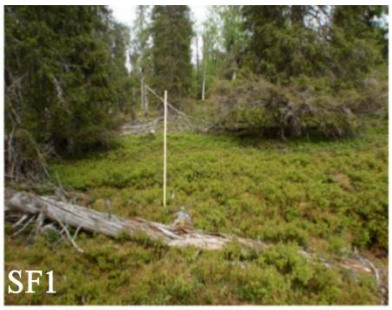
SF1


TZ1


OM2


SF2


FL1

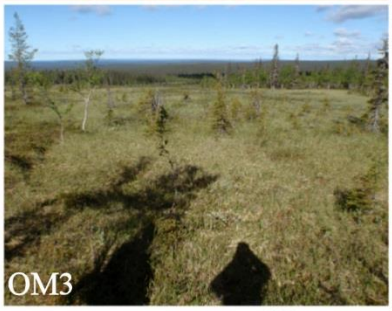
OM3


FL1


GC4/FL1

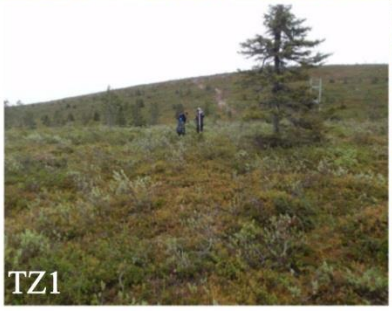
TZ1


TZ2

Observed variables:
P = precipitation (mm)
T_a = air temperature (°C)
Modeled variables:
P_r = rainfall (mm)
P_s = snowfall (mm)
SWE = snow water equivalent (mm)
M = melt (mm)
CC = cold content (mm)
LWHC = liquid water holding capacity (mm)
O = outflow (mm)

Adjusted parameters:
T_{crit} = threshold temperature for snowfall (°C)
CF_r = correction factor for rainfall (-)
T_m = threshold temperature for snowmelt (°C)
ddf (1 Sep) = degree day factor 1st of Sep (mm °C^{-1})
b = scaling factor for measured ddf (-)
TSF = surface temperature factor (-)
T_s = snow surface temperature (°C)
CCF = cold content degree day factor (mm°C^{-1})
f = maximum liquid water holding capacity (%)
Measured/calculated parameters:
ddf_{calc} = degree day factor (mm °C^{-1})
CF_s = correction factor for snowfall (-)

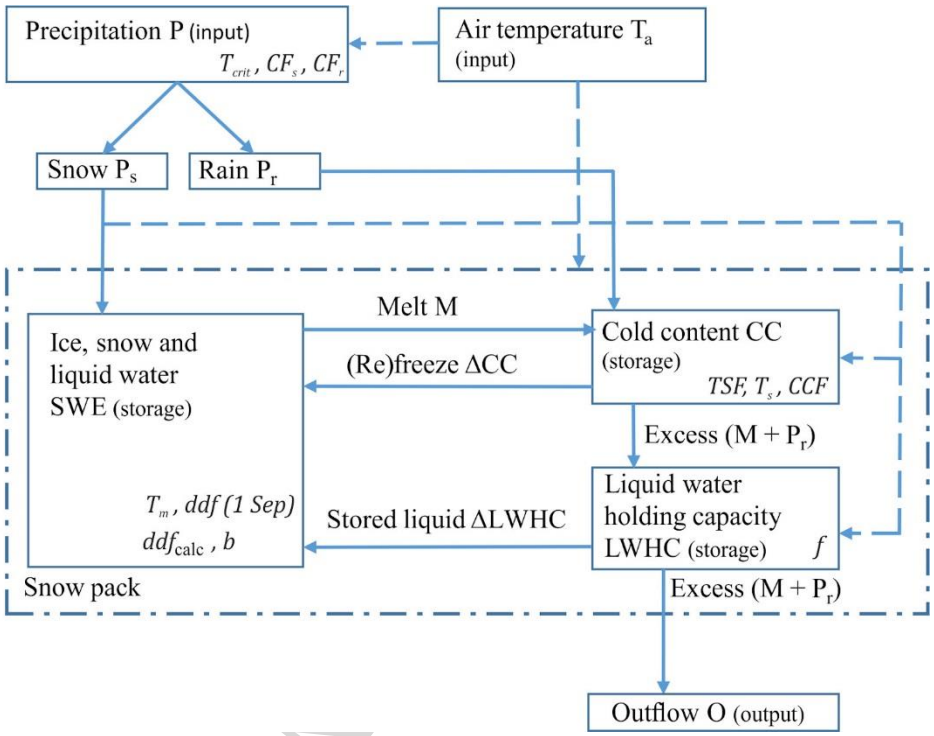

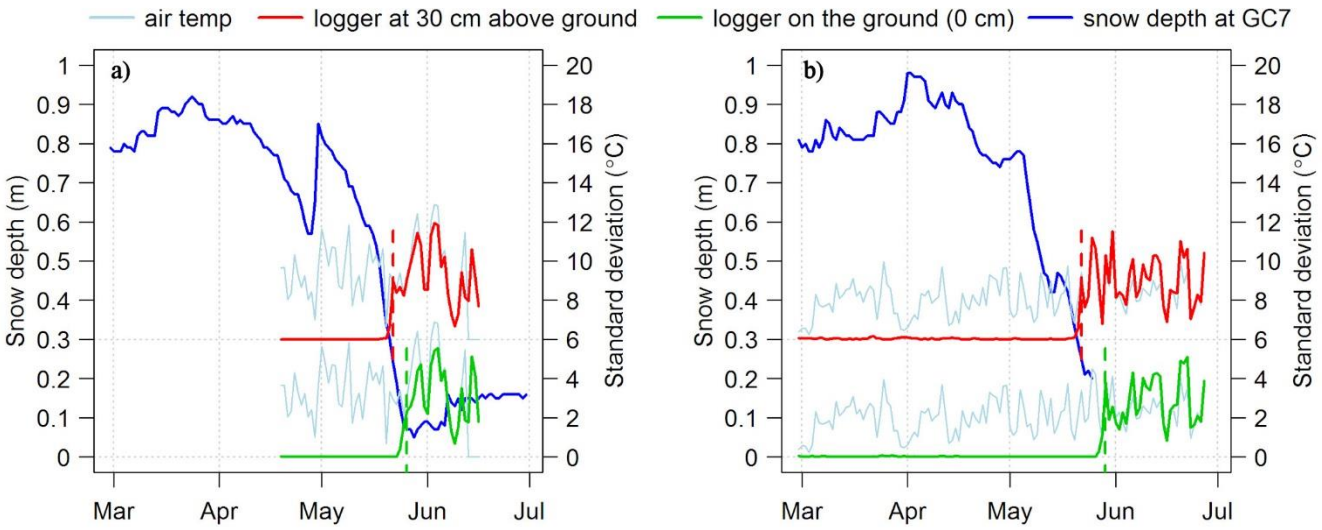

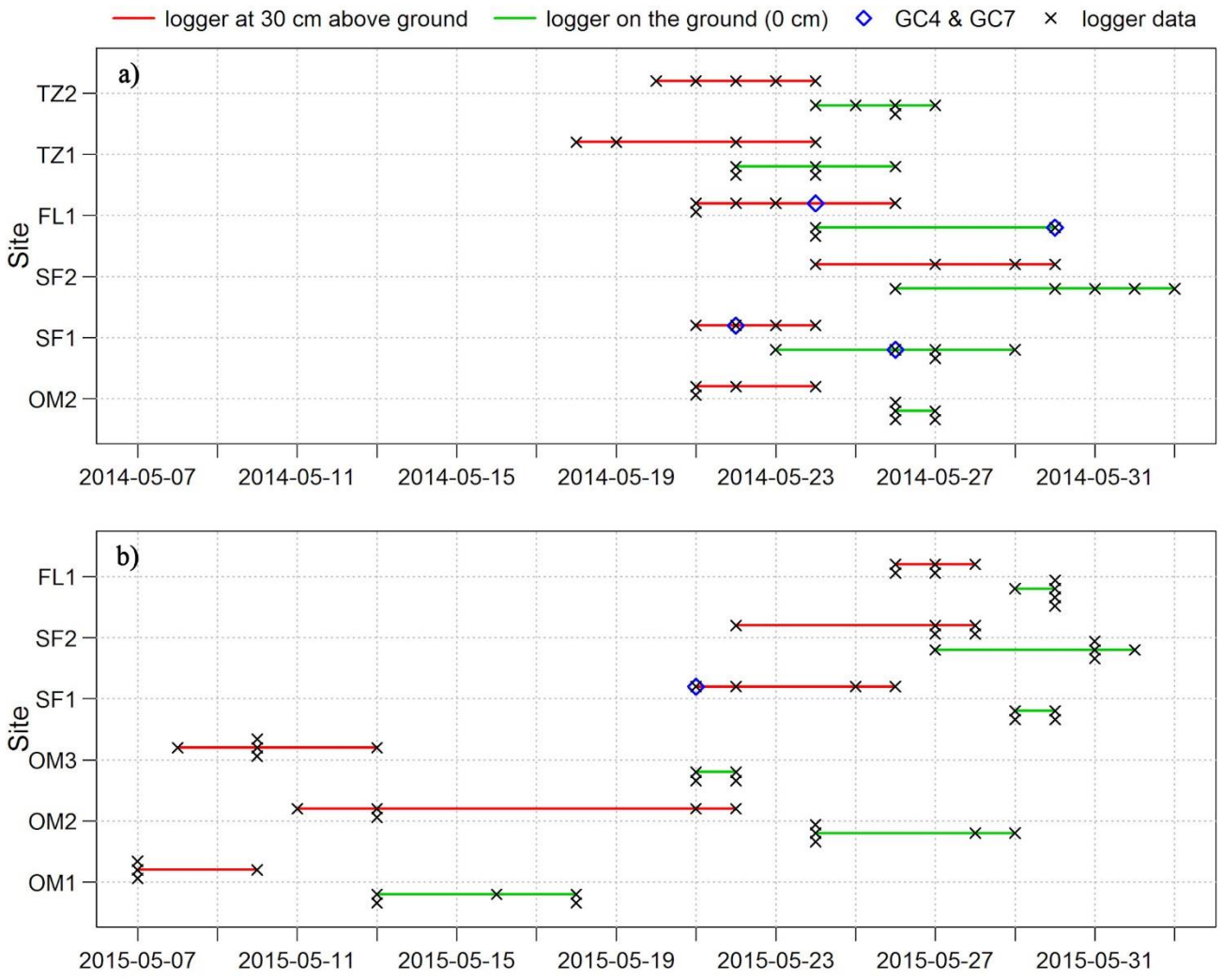

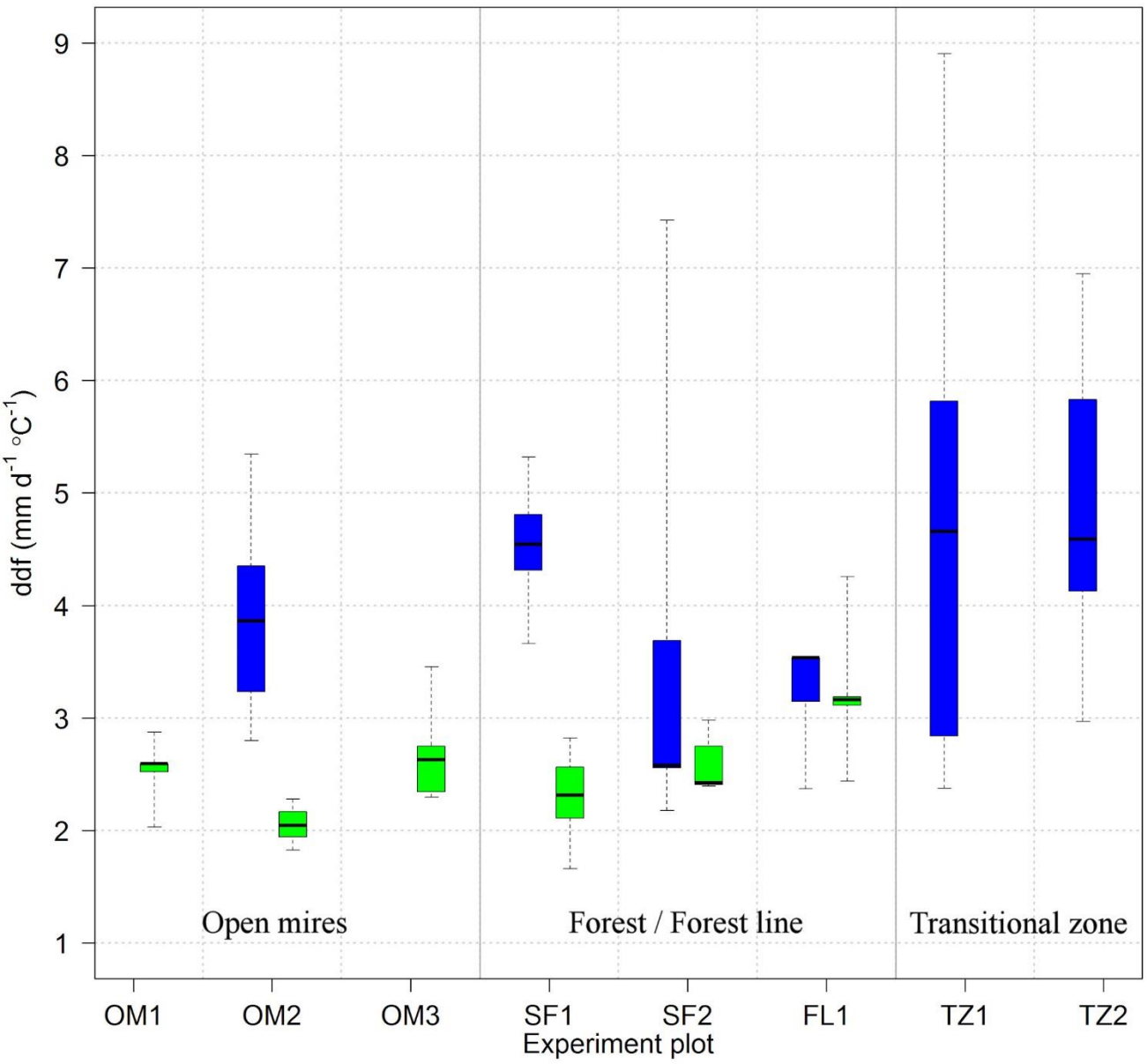

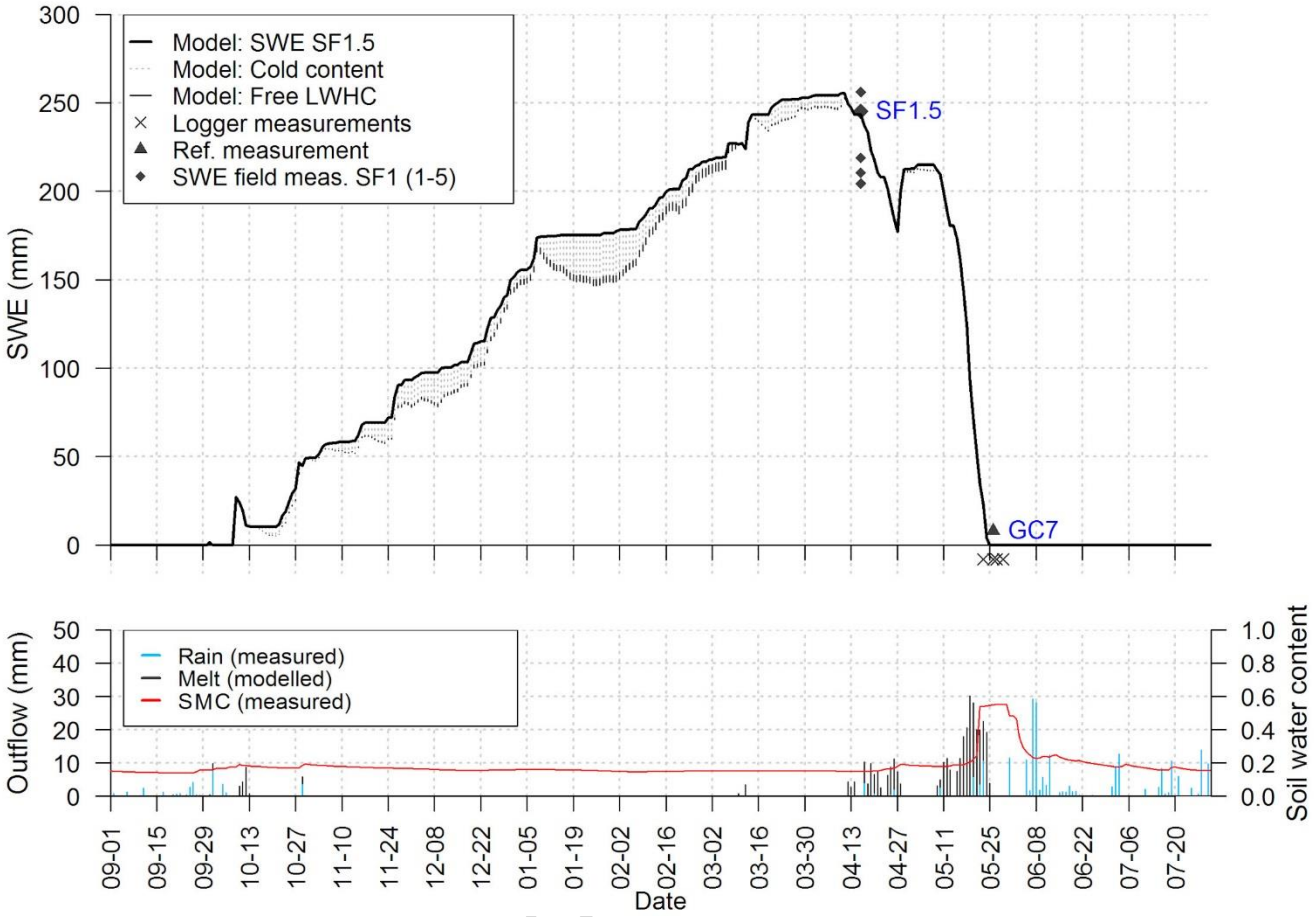

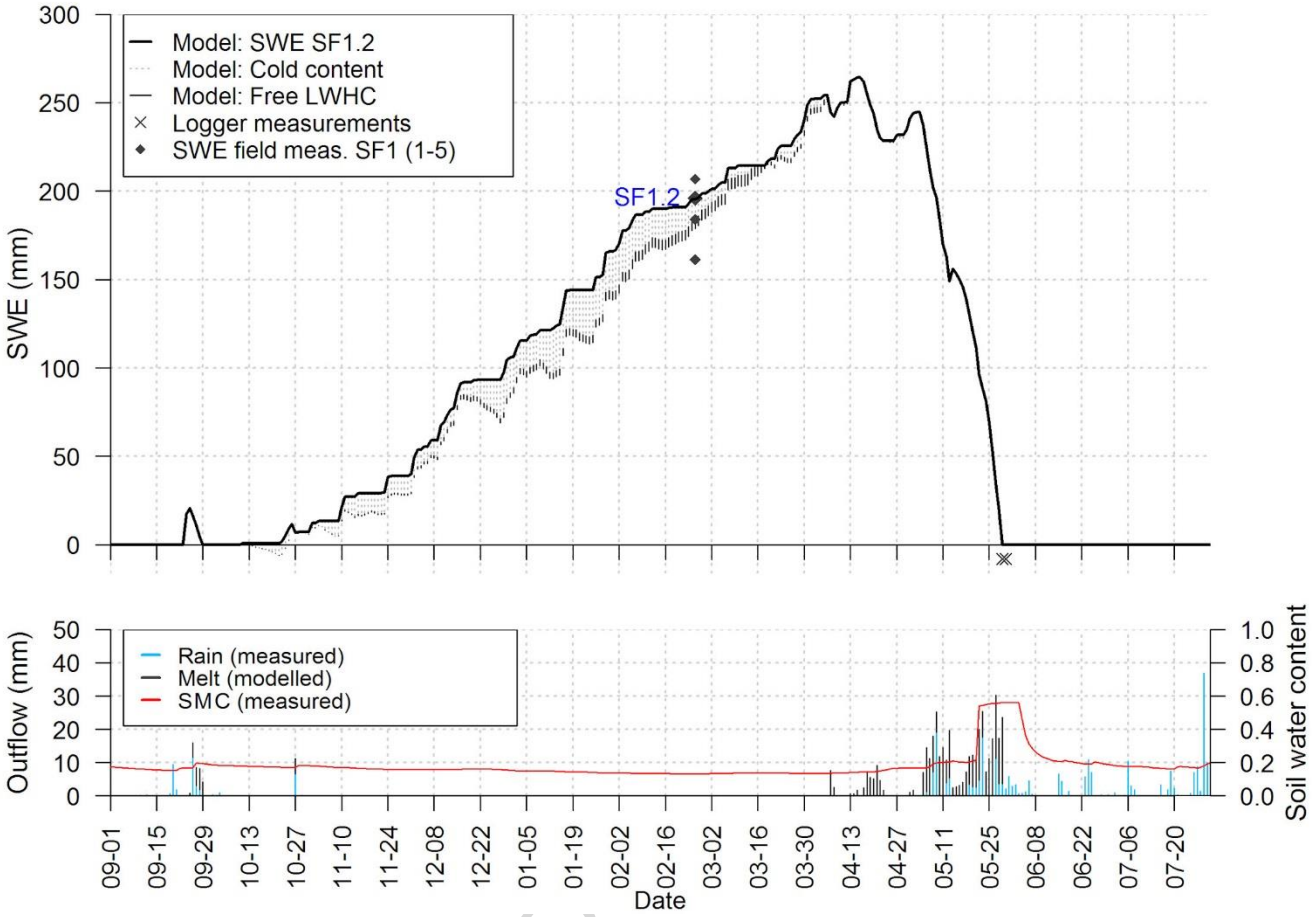

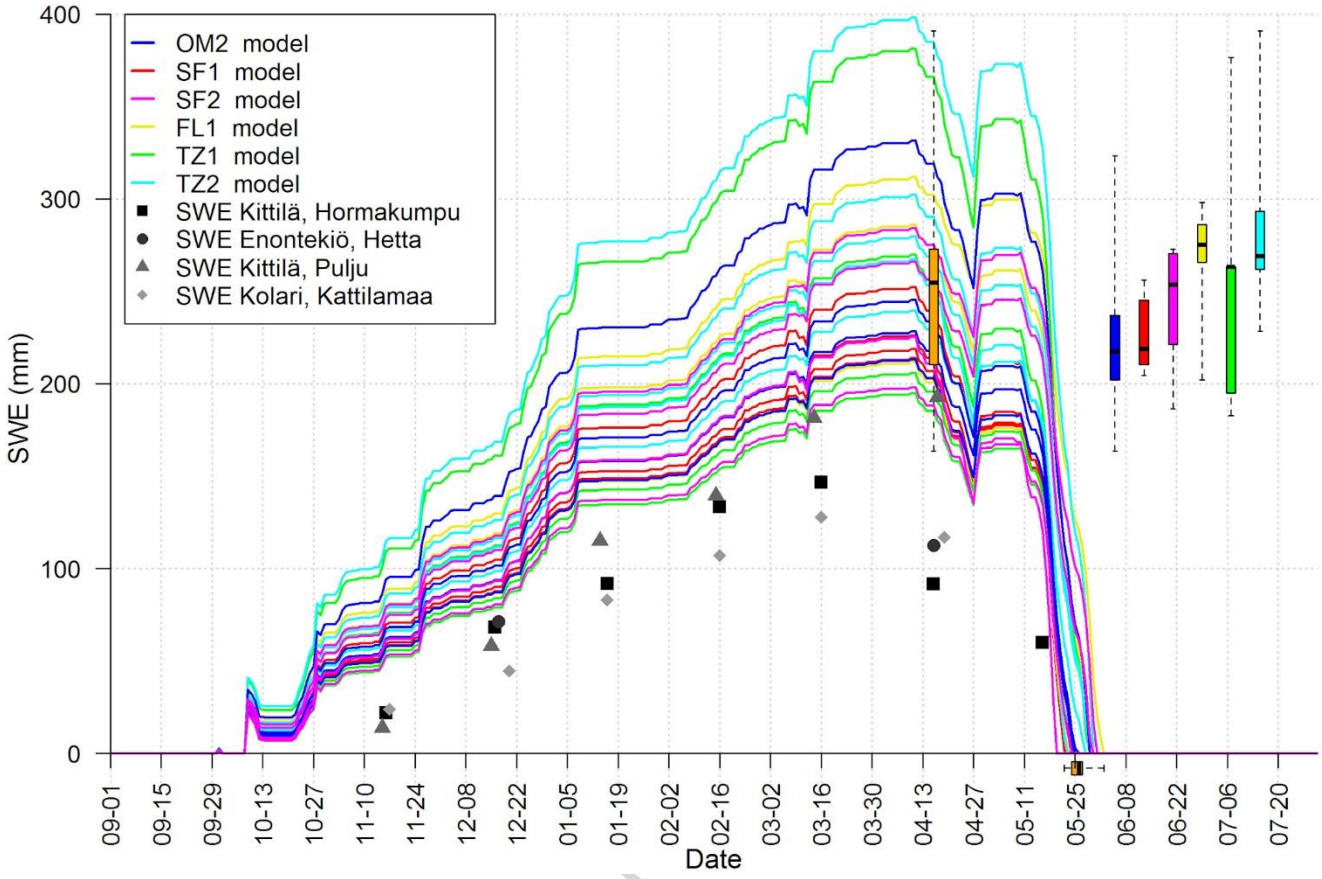

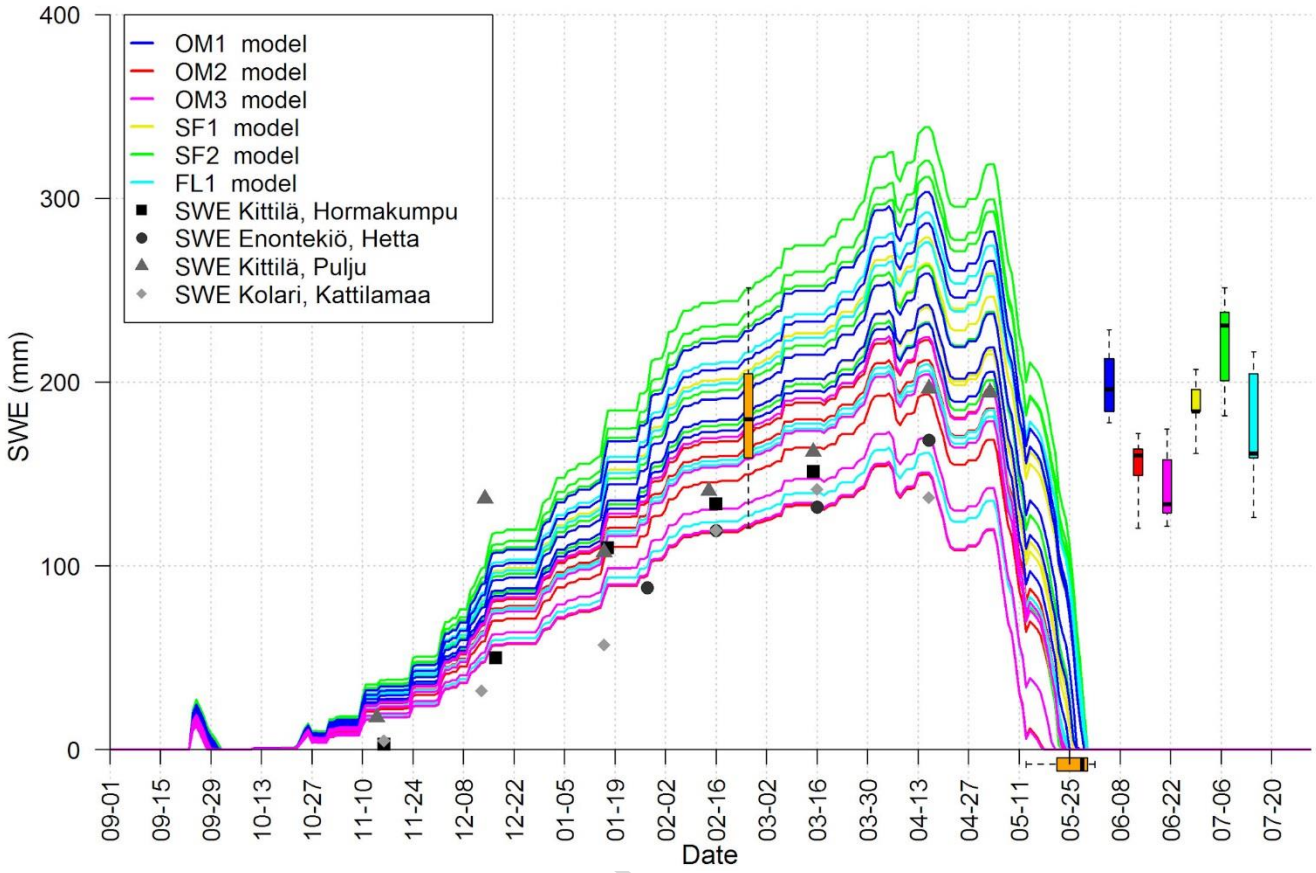

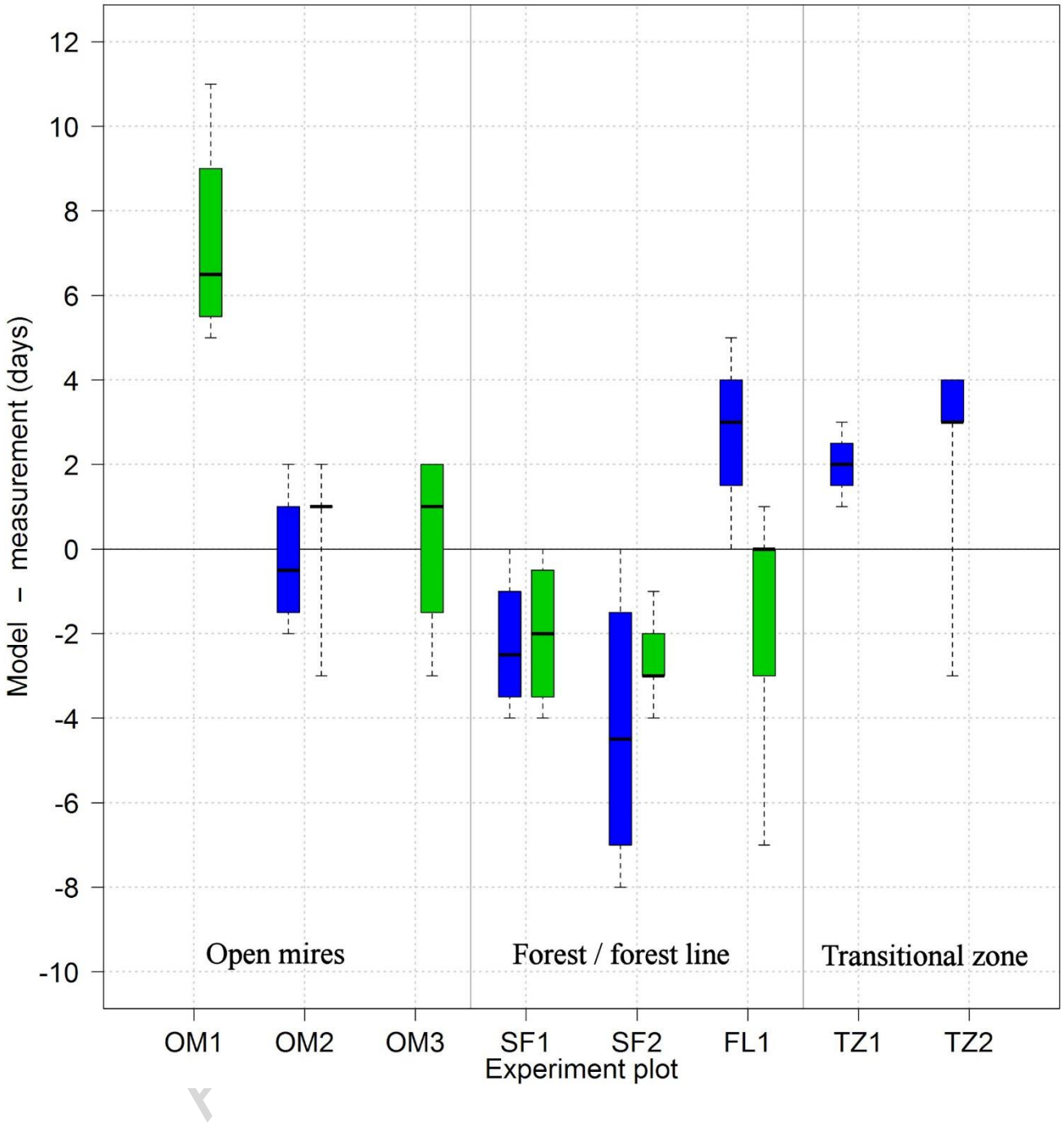

Highlights

- High-resolution temperature logging provides temporal and spatial data on snowmelt
- New algorithms estimate snowmelt process from snow profile temperature data
- Snowmelt rates showed high micro and local scale variability along a hillslope
- Snowmelt rates were successfully used in model parameterization
- On-line temperature logging increased the accuracy of the snow melt estimates